



Contents lists available at ScienceDirect

International Journal of Solids and Structures

journal homepage: www.elsevier.com/locate/ijsolstr

Non-linear wrinkling of a sandwich panel with functionally graded core – Extended high-order approach

Y. Frostig^a, V. Birman^b, G.A. Kardomateas^{c,*}

^a Ashrom Engineering Company Chair in Civil Engineering, Faculty of Civil and Environmental Engineering, Technion – Israel Institute of Technology, Haifa 32000, Israel

^b Department of Mechanical and Aerospace Engineering and Missouri S&T Global – Missouri University of Science and Technology, St. Louis, 12837 Flushing Meadows Dr., St. Louis, MO 63131, USA

^c School of Aerospace Engineering, Georgia Institute of Technology, Atlanta, GA 30332-0150, USA



ARTICLE INFO

Article history:

Revised 10 February 2018

Available online 14 February 2018

Keywords:

Sandwich panels

Wrinkling

Buckling

Functionally graded materials (FGM)

Extended high-order sandwich panel theory (EHSAPT)

Load control

Displacement control

Edge beam

ABSTRACT

The non-linear response of a sandwich panel with the core that consists of a functionally graded material (FGM) undergoing in-plane loading is investigated. The panel consists of two face sheets, metallic or composite laminated, and an FGM core that is a medium whose mechanical properties change through the depth facilitating a desirable response of the structure. The effect of the FGM core is introduced through the constitutive relations that affect conventional and high-order stress resultants and stress couples in the panel. The formulation employs the Extended High-Order Sandwich Panel Theory (EHSAPT) to assess the effect of the FGM material of the core. A variational approach is adopted to derive the linear and non-linear governing equations with a prescribed FGM distribution through the depth of the core. The wrinkling study of FGM panels includes two loading scenarios where in-plane loads are applied through a rigid edge beam connected to the core only and where the loads are applied through a rigid edge structure attached to both the face sheets and core causing uniform end shortening. The post-wrinkling behavior is also considered to prove that the initial pattern of wrinkles is not affected.

© 2018 Published by Elsevier Ltd.

1. Introduction

An ordinary sandwich panel consists of two face sheets and a core. Usually the face sheets are made of metallic or laminated composite materials and the core is made of either metallic or Nomex (metallized paper) honeycomb, low strength closed-cell or open-cell foam or balsa wood. The performance of such panel is significantly affected by the mechanical properties of the core. In customary design these properties are uniform through the depth of the homogeneous core, but they can be modified at selected regions in order to enhance the response, e.g., Frostig and Thomsen (2005) and Bozhevolnaya and Frostig (2006). In the last decades the use of FGM core for sandwich applications has emerged, e.g., Venkataraman and Sankar (2003), Apetre et al. (2008) and Birman and Vo (2017). In general, the FGM material is used to enhance the performance of structures through improvements of a variety of properties, such as stiffness, strength, thermal conductivity, residual stresses, delamination resistance, etc. In the case of sandwich panels, the FGM core consist of a material with a variable mass density (e.g., foam) or a composite material with

a variable content of the constituent phases (e.g., content of metal vs. ceramic) through the depth of the core. While such variations may enhance wrinkling stress and reduce delamination tendencies, other modes of failure, such as the strength of face sheets and global stability are little affected, unless the designer employs a heavy and stiff core that defies its purpose. Mathematically, a FGM core is modeled as a material with variable mechanical properties through the depth or over the planform of the panel. For example, Frostig and Thomsen (2008) considered thermal buckling and post-buckling of a sandwich panel where the properties of the core varied through the thickness due to the effect of a non-uniform temperature. The effect of a FGM core on the linear wrinkling instability and nonlinear post-wrinkling response of a sandwich panel is studied in this paper.

There are numerous applications where sandwich structures are subjected to in-plane compressive loads. Sandwich deck and bottom structures of ships are compressed as a result of bending in rough seas. Sandwich panels used as the bottom skin of the wings of an airplane are subjected to compression as a result of the bending moment produced by the weight of the wing and the engines carried by the wing. Among other wrinkling examples, though they are not analyzed here, are the dynamic wrinkling of a structure due to impact or vibrations produced by unbalanced machinery, and the thermal wrinkling caused by an elevated

* Corresponding author.

E-mail address: george.kardomateas@aerospace.gatech.edu (G.A. Kardomateas).

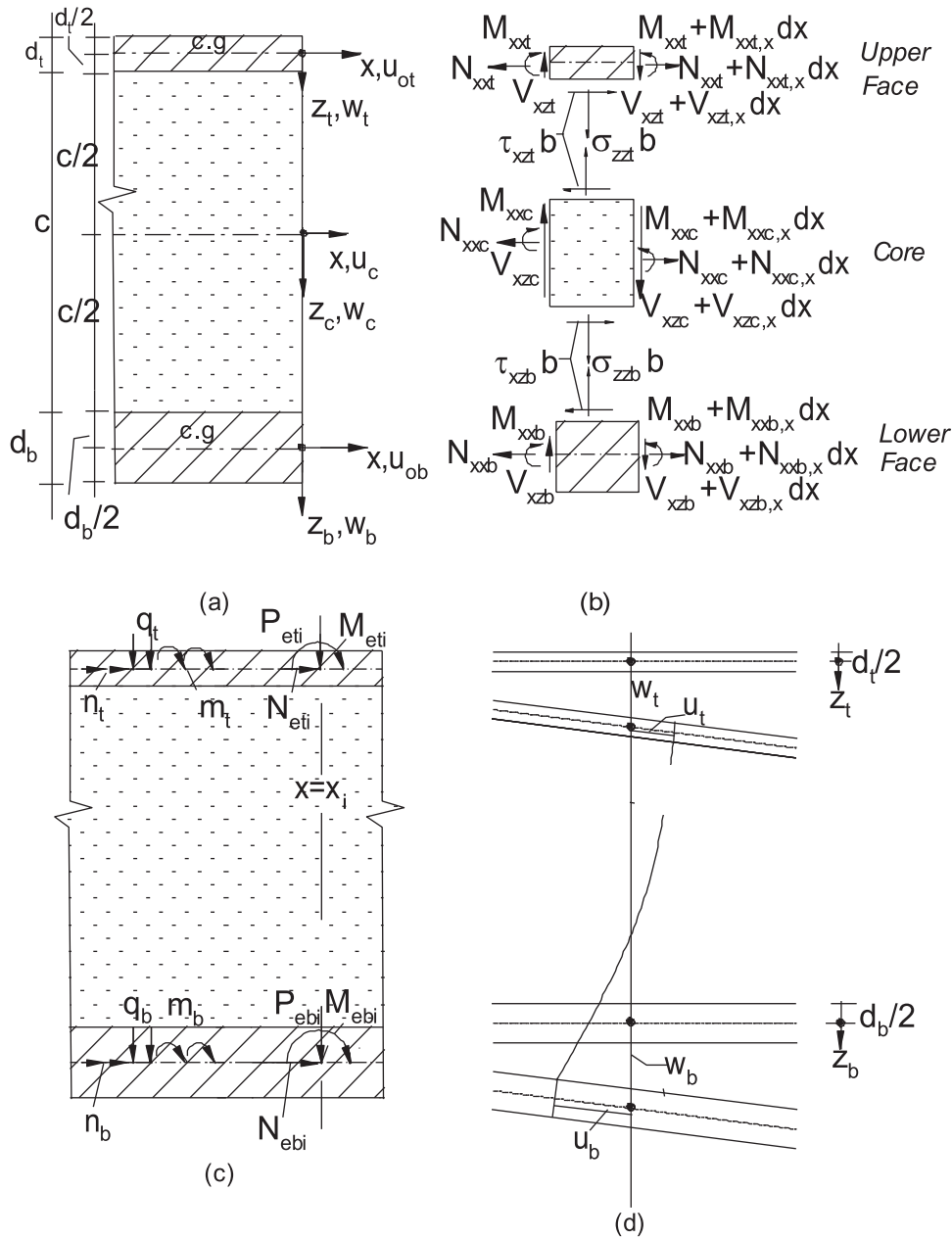


Fig. 1. Sign convention and geometry: (a) coordinate system, (b) stress resultants, (c) loads (c) and (d) displacement pattern through the depth of sandwich panel.

temperature that may be combined with static compression. Additionally, one of the facings of any sandwich structure experiencing bending is compressed and can wrinkle, even though the opposite facing is in tension.

A recent paper on the effect of functional grading of the core on wrinkling stability of sandwich panels demonstrated the effectiveness of a graded core (Birman and Vo, 2017). By concentrating denser thin core layers adjacent to the face sheets, the wrinkling stress was increased by several times. Furthermore, it was shown that while the wrinkling stress is reduced under uniform temperature in both homogeneous and graded core panels, the improvement achieved through grading is preserved.

Analyses of sandwich panels utilize two main approaches. The first assumes that the cores are very stiff, i.e. incompressible, in the vertical (thickness) direction and possess negligible in-plane rigidity in the in-plane directions (metallic or Nomex honeycomb is a representative example of such cores). Examples of the analyses utilizing this approach can be found in the textbooks by Allen

(1969), Plantema (1966) and Vinson (1999). Such panels can be modeled by the First-Order (e.g., Mindlin, 1951), or High-Order shear deformation theories (e.g., Reddy, 1999) that represent the incompressible core as an equivalent single layer, ESL. The second, also referred to as layer-wise approach, depends on High-Order models, see for example Frostig et al. (1992) that obtained the solution for the core fields in a closed-form or Carrera and Brischetto (2009) that presumed the displacements fields of the core. In such models the overall response is derived using the responses of the face sheets and the core subject to the equilibrium and compatibility requirements.

The High-Order approach where the in-plane rigidity of the core is neglected has been considered by Frostig and others using the High-Order Sandwich Panel Theory (HSAPT). This approach has been extensively employed in static, dynamic, linear and non-linear applications, e.g., beam analysis by Frostig et al. (1992); buckling and free vibration by Frostig and Baruch (1993, 1994); non-linear behavior by Sokolinsky and Frostig (2000); dynamic re-

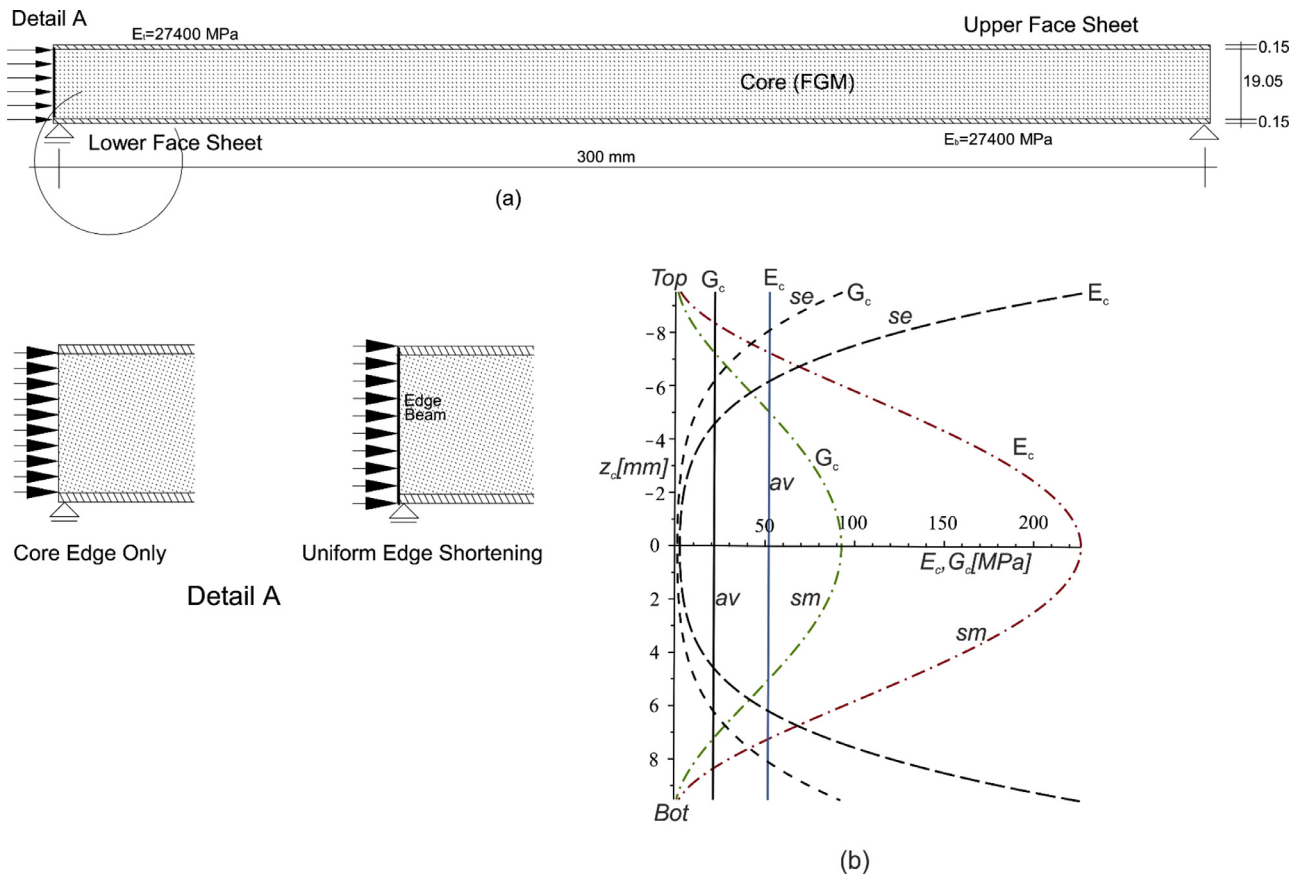


Fig. 2. Sandwich panel: (a) geometry and load transfer mechanism (Detail A), (b) FGM properties distribution through the depth of core.

sponse of debonded panels by Schwarts-Givli et al. (2007a, 2007b) and free vibration with thermal effects by Frostig and Thomsen (2009a, 2009b).

In the case where a finite in-plane core rigidity has to be considered, such as in medium to heavy mass density foam or wood or if the response of the panel is of a local nature, such as wrinkling, an enhanced model referred to as EHSAPT has been implemented. It represents an extension of the HSAPT model and employs the closed-form polynomial displacement field distributions through the depth of the core. This theory has been applied to a number of problems. In particular, Frostig (2011) applied EHSAPT to the analysis of in-plane loads through core, Phan et al. (2012a, 2012b) studied wrinkling and global buckling of sandwich panels, Phan et al. (2012c) considered free vibrations and Frostig et al. (2016) studied curved sandwich panels. Recently the enhanced model has been implemented in a special finite element by Yuan et al. (2015).

It is worth mentioning that while the exploration of FGM in sandwich structures is a relatively new area, biological tissues have always been functionally graded. One of the examples of grading is found in the tendon-to-bone insertion (enthesis) where a huge mismatch of the stiffness occurs between tendon and bone over a short distance of less than 1 mm (Genin et al., 2009). In this case the combination of the gradient of collagen (protein) fiber orientation combined with the gradient in the mineral content from bone to tendon results in a relatively compliant band within the insertion site. It has been suggested that the function of such rather unexpected compliance is a higher toughness of the joint. Another biomedical example of grading is found in human sclera where the orientation and distribution of collagen fibers yields an enhanced response (Pijanka et al., 2012). In engineering FGM have been considered for numerous applications since they were first proposed

for thermal barrier coatings in 1980th (Koizumi 1997). A detailed review of FGM studies is outside the scope of this paper; reviews and sources of information on these materials can be found in Suresh and Mortensen (1998), Miyamoto (1999), Birman and Byrd (2007), Paulino (2008), Birman et al. (2012) and Birman (2014). A spectrum of problems that have to be addressed to utilize the advantages of FGM includes manufacturability, micromechanic modeling establishing the properties as functions of local content of constituent materials and topology, heat and moisture transfer (if the material is employed in hydrothermal environments), the formulation of governing equations and boundary conditions, and stress, stability or dynamic analysis. The solution of fracture problems is also often necessitated (e.g., Dodds et al., 2002). Notably, the problems relevant to FGM are often coupled. For example, local thermal conductivity may be affected by local temperature. However, the solution of the heat transfer problem depends on the conductivity, so that the heat transfer and micromechanics solutions cannot be separated.

In this paper the governing equations and the appropriate boundary conditions for a sandwich panel where the core properties are coordinate-dependent are derived explicitly. The mathematical formulation follows the steps of the Enhanced High-Order Theory (EHSAPT) developed by Phan et al. (2012a). This theory has been proven to be very accurate by comparing to elasticity for static transverse loading in Phan et al. (2012b); for global buckling behavior in Phan et al. (2012a); for wrinkling behavior in Phan et al. (2012c); and for dynamic loading in Phan et al. (2013). The benchmark elasticity solutions for sandwich beams/wide plates were developed for wrinkling in Kardomateas (2005); for global buckling in Kardomateas (2010); for static transverse loading in Kardomateas and Phan (2011) and for dynamic loading in Kardomateas et al. (2013). The effects of

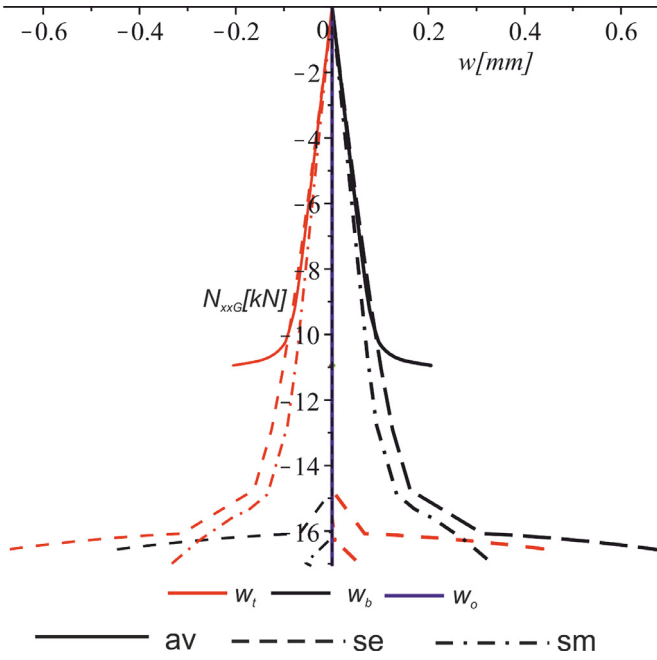


Fig. 3. Extreme vertical displacement as a function of the compressive force generated Load Displacement control at the edge $x=0$ subject to a controlled displacement.

the FGM heterogeneous mechanical properties through the depth of the core on the wrinkling behavior of the panel are accounted for. The sandwich face sheets are assumed linearly elastic and undergoing large displacements with moderate rotations and small strains. The core is linear in both physical (linear elasticity) and geometric sense (linear strain-displacement relationships). Contrary to High-Order theories, the core possesses finite stiffness in all planes, including in-plane stiffness, normal stiffness in the direction perpendicular to the middle plane as well as finite shear rigidities in the middle plane and in the planes perpendicular to the middle plane. It is assumed that perfect bonding exists between the face sheets and the core at their interfaces and the loads may be applied both to the core (with the specifics discussed below) and to the face sheets.

The mathematical formulation of the EHSAPT computational model accounting for the FGM properties of the core is followed with a numerical study of two basic cases. In the first case the in-plane loads are applied to the core through a rigid edge beam extended through the thickness of the core, while in the second the edge displacements are applied through a rigid edge beam extended through the entire depth of the sandwich panel yielding a uniform end shortening. The former case can be referred to as “controlled force,” while the latter case represents “controlled displacement.” A significant difference in the response of the sandwich panel to these two loading cases is discussed in detail, including its implication to design of sandwich joints. Two symmetric types of FGM distributions are considered with the enhanced stiffness either in the vicinity to core-face interfaces or around the middle plane of the core.

2. Mathematical formulation

The mathematical formulation employs the EHSAPT (Extended High-Order Sandwich Panel Theory) model to derive the field equations and the appropriate boundary conditions, see Frostig (2011) for more details. The sandwich panel, its geometry and coordinate system employed in the subsequent analysis are depicted in Figs. 1 and 2. In the following, the face sheets are assumed homogeneous and isotropic, while the core is heteroge-

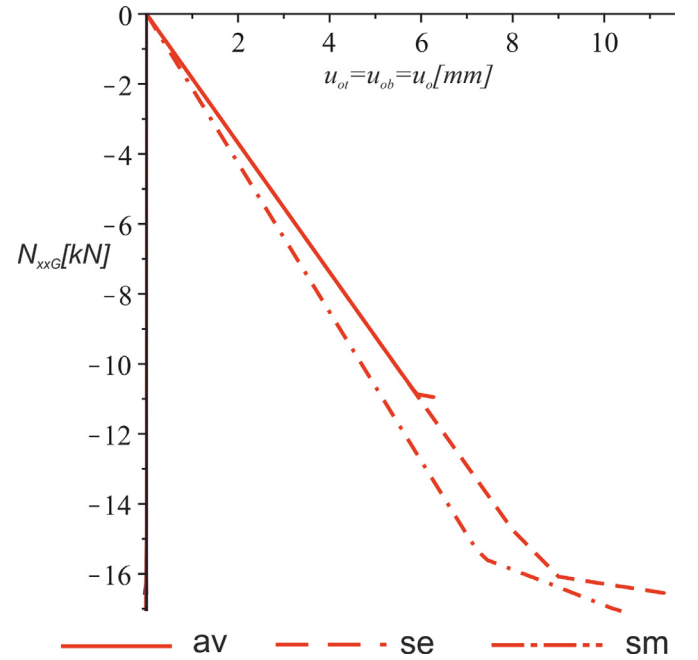


Fig. 4. Relationship between the maximum longitudinal controlled displacement at $x=0$ and the resulting compressive force.

neous and quasi-isotropic, i.e. its properties vary through the thickness, but they remain isotropic at each location. The generalization for the case of composite face sheets would not present any complications. The forces and moments referred to below are applied in the cross sections perpendicular to the x -axis, i.e. there are no forces and moments acting out of plane in Fig. 1.

The governing equations and the boundary conditions are derived via the variational principle imposed on the total potential energy:

$$\delta(U + V) = 0 \quad (1)$$

where U and V are the internal and the external potential energy, respectively, and δ denotes the variation operator.

The internal potential energy is

$$\begin{aligned} \delta U = & \int_{V_t} \sigma_{xxt} \delta \varepsilon_{xxt} dV + \int_{V_b} \sigma_{xxb} \delta \varepsilon_{xxb} dV \\ & + \int_{V_c} (\tau_{xzc} \delta \gamma_{xzc} + \sigma_{xxc} \delta \varepsilon_{xxc} + \sigma_{zcc} \delta \varepsilon_{zcc}) dV \end{aligned} \quad (2)$$

where σ_{xxj} and ε_{xxj} ($j=t,b,c$) are the in-plane normal stresses and strains in the upper and the lower face sheets and the core, respectively, τ_{xzc} and γ_{xzc} are the transverse shear stresses and strains in the core, and σ_{zcc} and ε_{zcc} are the normal stresses and strains in the vertical (thickness) direction of the core.

The external potential energy is given by

$$\begin{aligned} \delta V = & - \int_0^L (n_t \delta u_{ot} + q_t \delta w_t + m_t \delta w_{t,x} + n_b \delta u_{ob} + q_b \delta w_b \\ & + m_b \delta w_{b,x}) dx - \sum_{i=1}^{NC} \int_0^L [N_{eti} \delta u_{ot} + P_{eti} \delta w_t + M_{eti} \delta w_{t,x} + N_{ebi} \delta u_{ob} \\ & + P_{ebi} \delta w_b + M_{ebi} \delta w_{b,x} + N_{eci} \delta u_c (z_c = z_{cgc}) + P_{eci} \delta w_c (z_c = z_{cgc}) \\ & + M_{eci} \delta (w_{c,x}) (z_c = z_{cgc})] \delta_d (x - x_i) dx \end{aligned} \quad (3)$$

where n_j , q_j and m_j ($j=t,b$) are the in-plane and vertical distributed loads and the bending moment distributed loads respectively (see Fig. 1); N_{eji} , P_{eki} and M_{eji} ($j=t,b,c$) are external concentrated loads

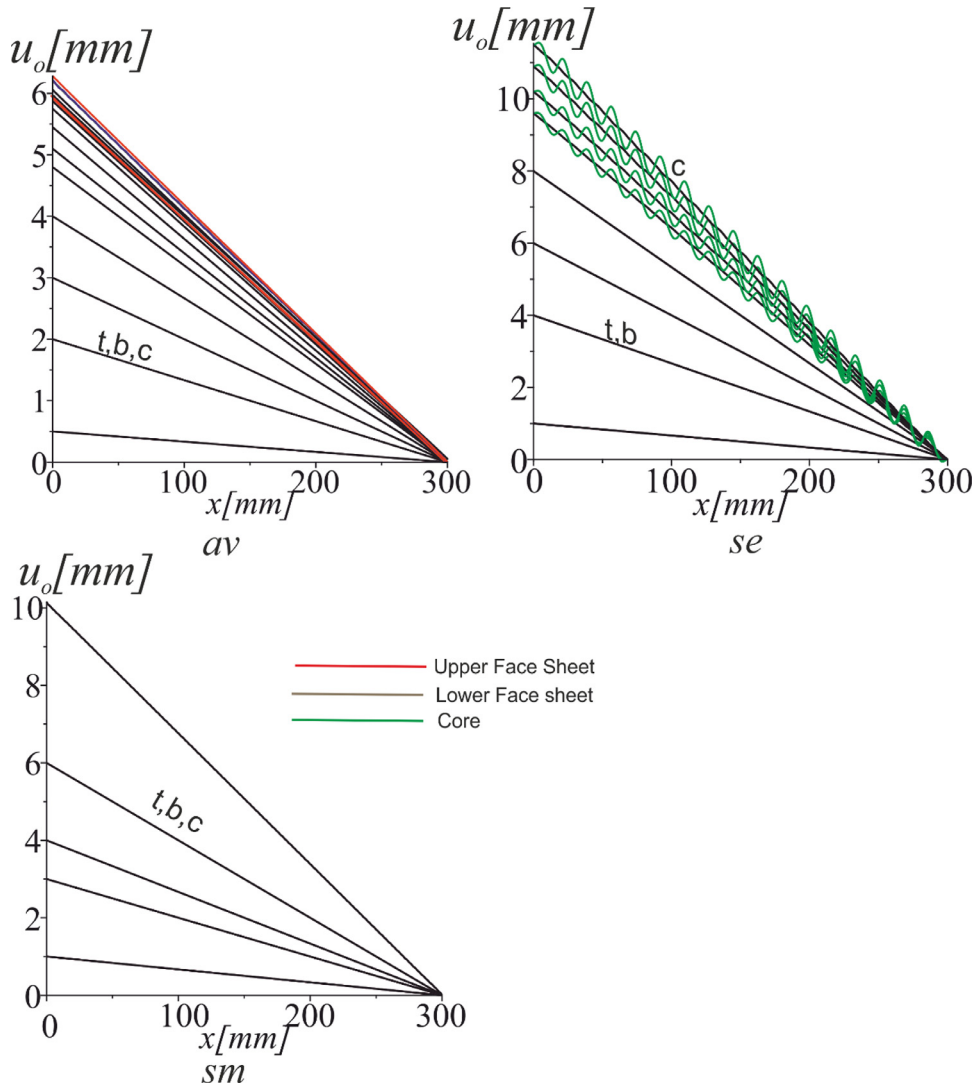


Fig. 5. Longitudinal displacements along the middle plane of the sandwich panel prior to and after wrinkling for loading that is controlled displacement at the left end ($x=0$).

in the in-plane and vertical directions and the concentrated moment respectively exerted at $x = x_i$ on the face sheets and at the centroid of the core (at $z_c = z_{cgc}$), u_{oj} , w_j and $w_{j,c}$ ($j = t, b, c$) are the longitudinal and vertical displacements and rotation at the centroid of the face sheets and the core respectively, NC denotes the number of concentrated loads; $\delta_d(x-x_i)$ is the delta Dirac function; u_{oj} , w_j and $w_{j,x}$ ($j = t, b$) are the in-plane and vertical displacements and the rotation of each face sheet, x is the longitudinal coordinate and L is the length of the panel. Detailed geometry and sign convention of stresses, displacements, and loads are depicted in Fig. 1.

The field equations are derived through the introduction of the displacement fields and strains in the face sheets and core and applying the compatibility conditions along the face sheet – core interfaces as follows.

The displacement and strain pattern in the face sheets ($j = t, b$) is specified following the Bernoulli assumption and using the strain-displacement relations for moderate displacements:

$$\begin{aligned} u_j(x, z_j) &= u_{oj}(x) - z_j \frac{d}{dx} w_j(x) \\ \varepsilon_j(x, z_j) &= \varepsilon_{oj}(x) - z_j \chi_j(x) \end{aligned} \quad (4)$$

In (4), the middle plane in-plane strains and curvatures are

$$\varepsilon_{oj}(x) = \frac{d}{dx} u_{oj}(x) + 1/2 \left(\frac{d}{dx} w_j(x) \right)^2, \quad \chi_j(x) = \frac{d^2}{dx^2} w_j(x) \quad (5)$$

and z_j ($j = t, b$) are the vertical coordinates of each face sheet measured downwards from the centroid of the corresponding face (Fig. 1).

The displacement pattern of the core is non-linear coinciding with its counterpart in the HSAPT model (Frostig et al., 1992):

$$u_c(x, z_c) = u_o(x) + u_1(x)z_c + u_2(x)z_c^2 + u_3(x)z_c^3 \quad (6)$$

$$w_c(x, z_c) = w_o(x) + w_1(x)z_c + w_2(x)z_c^2$$

where z_c is the vertical coordinate within the core, measured from the middle plane downwards, and $u_k(x)$ ($k=0,1,2,3$) and $w_k(x)$ ($k=0,1,2$) are unknown functions. Hence, the geometrically linear strain-displacement relations in the core read:

$$\begin{aligned} \varepsilon_{xzc}(x, z_c) &= \frac{d}{dx} u_o(x) + \left(\frac{d}{dx} u_1(x) \right) z_c + \left(\frac{d}{dx} u_2(x) \right) z_c^2 + \left(\frac{d}{dx} u_3(x) \right) z_c^3 \\ \varepsilon_{zxc}(x, z_c) &= w_1(x) + 2w_2(x)z_c \\ \gamma_{zxc}(x, z_c) &= u_1(x) + 2u_2(x)z_c + 3u_3(x)z_c^2 + \frac{d}{dx} w_o(x) \\ &\quad + \left(\frac{d}{dx} w_1(x) \right) z_c + \left(\frac{d}{dx} w_2(x) \right) z_c^2 \end{aligned} \quad (7)$$

where ε_{xzc} , ε_{zxc} and γ_{zxc} are the normal strains in the longitudinal and vertical directions, and the transverse shear strain, respectively.

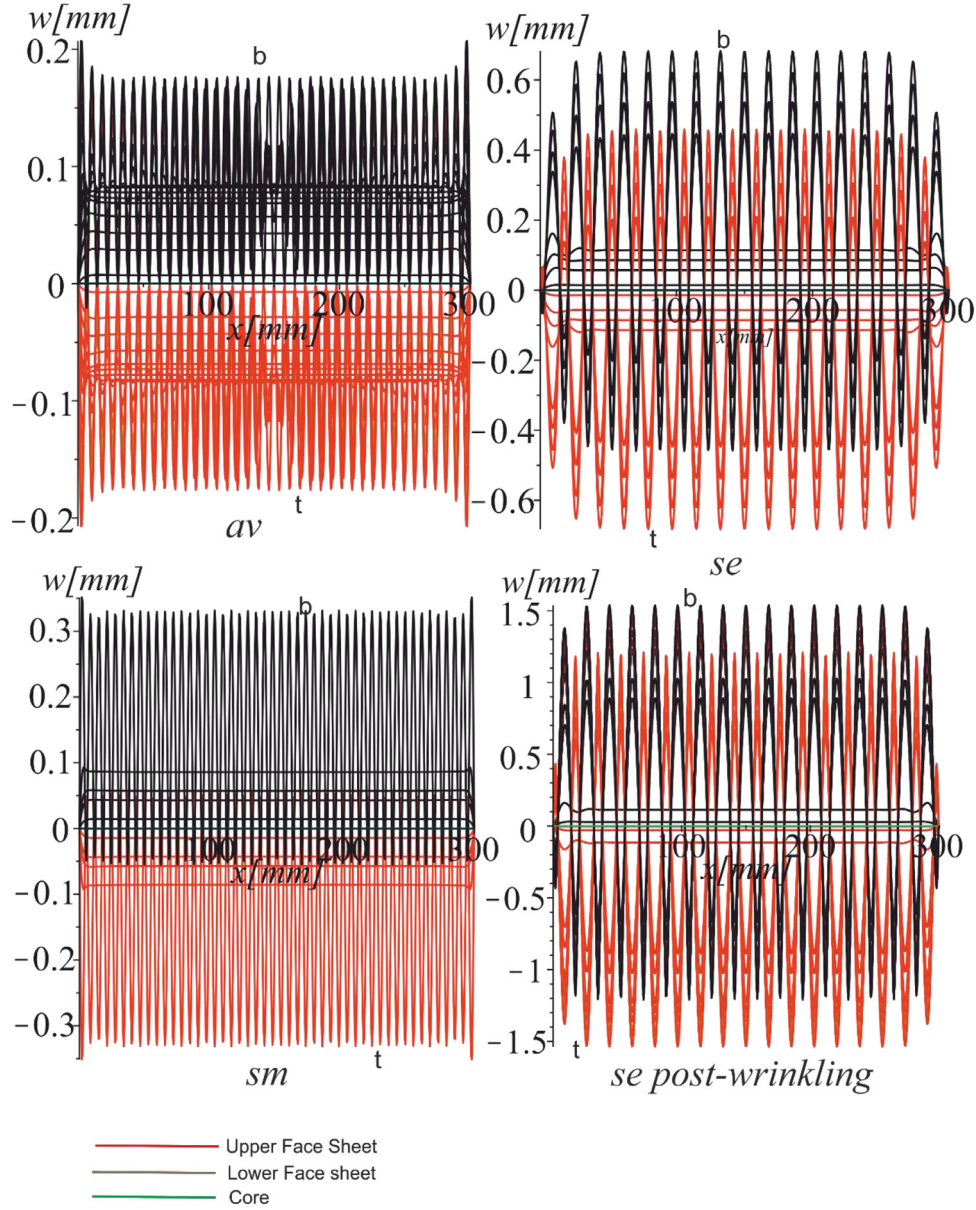


Fig. 6. Vertical displacements of the top and lower facings along the span of the sandwich beam subject to controlled axial displacement.

The compatibility conditions at the upper and the lower face sheet–core interfaces are formulated using the first equation Eq. (4):

$$u_c\left(x, -\frac{1}{2}c\right) = u_{ot}(x) - \frac{1}{2}\left(\frac{d}{dx}w_t(x)\right)d_t, \quad w_c\left(x, -\frac{1}{2}c\right) = w_t(x)$$

$$u_c\left(x, \frac{1}{2}c\right) = u_{ob}(x) - \frac{1}{2}\left(\frac{d}{dx}w_b(x)\right)d_t, \quad w_c\left(x, \frac{1}{2}c\right) = w_b(x)$$
(8)

The use of these conditions along with the displacements of the core given by Eq. (6) enables us to express four out of seven unknown functions of the displacement pattern of the core:

$$w_1(x) = \frac{-w_t(x) + w_b(x)}{c}, \quad w_2(x) = \frac{2(w_t(x) - 2w_o(x) + w_b(x))}{c^2}$$

$$u_2(x) = \frac{2u_{ot}(x) - \left(\frac{d}{dx}w_t(x)\right)d_t + 2u_{ob}(x) + \left(\frac{d}{dx}w_b(x)\right)d_b - 4u_o(x)}{c^2}$$

$$u_3(x) = \frac{2(-2u_{ot}(x) + \left(\frac{d}{dx}w_t(x)\right)d_t - 2u_1(x)c + 2u_{ob}(x) + \left(\frac{d}{dx}w_b(x)\right)d_b)}{c^3}$$
(9)

This leaves three unknown functions in the core and two unknown functions in each of two face sheets that will be determined from the variational principle.

The field equations are now derived using the variational principle, Eq. (1). The substitution of the strains in the face sheets and the core utilizing Eqs. (4) and (7) in Eqs. (2) and (3) and using the compatibility conditions in Eq. (9) yields

$$\frac{d}{dx}N_{xxt}(x) = 4\frac{M_{xz1c}(x)}{c^2} - 12\frac{M_{xz2c}(x)}{c^3} - n_t$$

$$\frac{d}{dx}V_{xzt}(x) = 4\frac{M_{zzc}(x)}{c^2} - \frac{R_{zzc}(x)}{c} - q_t$$

$$\frac{d}{dx}M_{xxt}(x) = V_{xzt}(x) - N_{xt}(x)\frac{d}{dx}w_t(x) - 2\frac{M_{xz2c}(x)}{c^2} + \frac{M_{xz1c}(x)}{c}$$

$$+ m_t(x) - 6\frac{M_{xz2c}(x)d_t}{c^3} + 2\frac{M_{xz1c}(x)d_t}{c^2}$$

$$\frac{d}{dx}N_{xxe}(x) = 12\frac{M_{xz2c}(x)}{c^3} + 4\frac{M_{xz1c}(x)}{c^2} - n_b$$

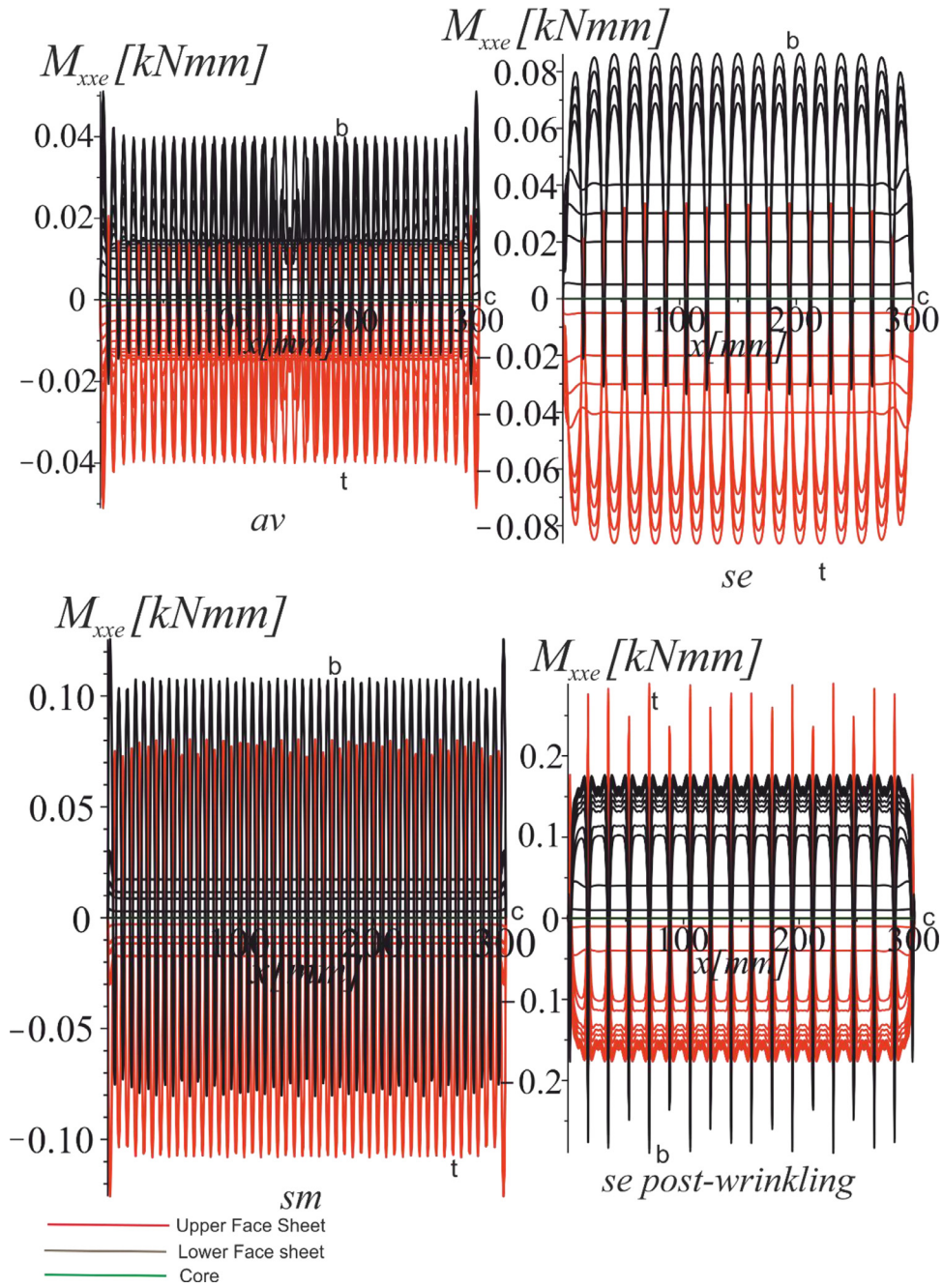


Fig. 7. Bending moment upon wrinkling along the span of the sandwich beam subject to controlled displacement.

$$\begin{aligned}
 \frac{d}{dx} V_{xzeb}(x) &= 4 \frac{M_{zzc}(x)}{c^2} + \frac{R_{zzc}(x)}{c} - q_b \\
 \frac{d}{dx} M_{xxeb}(x) &= V_{xzeb}(x) - \frac{M_{xz1c}(x)}{c} - N_{xxb}(x) \frac{d}{dx} w_b(x) - 2 \frac{M_{xz2c}(x)}{c^2} \\
 &\quad + m_b(x) - 2 \frac{d_b M_{xz1c}(x)}{c^2} - 6 \frac{M_{xz2c}(x) d_b}{c^3} \\
 \frac{d}{dx} N_{xxec}(x) &= -8 \frac{M_{xz1c}(x)}{c^2} \\
 \frac{d}{dx} M_{xxec}(x) &= V_{xzec}(x) - 8 \frac{M_{xz2c}(x)}{c^2} \\
 \frac{d}{dx} V_{zxec}(x) &= -8 \frac{M_{zzc}(x)}{c^2}
 \end{aligned}
 \tag{10}$$

Equivalent stress resultants and couples that appear in Eq. (10) account for the contribution of the high-order stress resultants and couples of the core:

$$\begin{aligned}
 N_{xxet}(x) &= N_{xxt}(x) - 4 \frac{M_{xx3c}(x)}{c^3} + 2 \frac{M_{xx2c}(x)}{c^2} \\
 M_{xxet}(x) &= -M_{xxt}(x) + 2 \frac{M_{xx3c}(x) d_t}{c^3} - \frac{M_{xx2c}(x) d_t}{c^2} \\
 V_{zzet}(x) &= \\
 &\quad \left(\frac{d}{dx} M_{xx2c}(x) \right) d_t c - 2 \left(\frac{d}{dx} M_{xx3c}(x) \right) d_t + \left(\frac{d}{dx} M_{xxt}(x) \right) c^3 \\
 &\quad + \frac{N_{xxt}(x) \left(\frac{d}{dx} w_t(x) \right) c^3 - c(c + 2d_t) M_{xz1c}(x) + (2c + 6d_t) M_{xz2c}(x) - m_t(x) c^3}{c^3}
 \end{aligned}$$

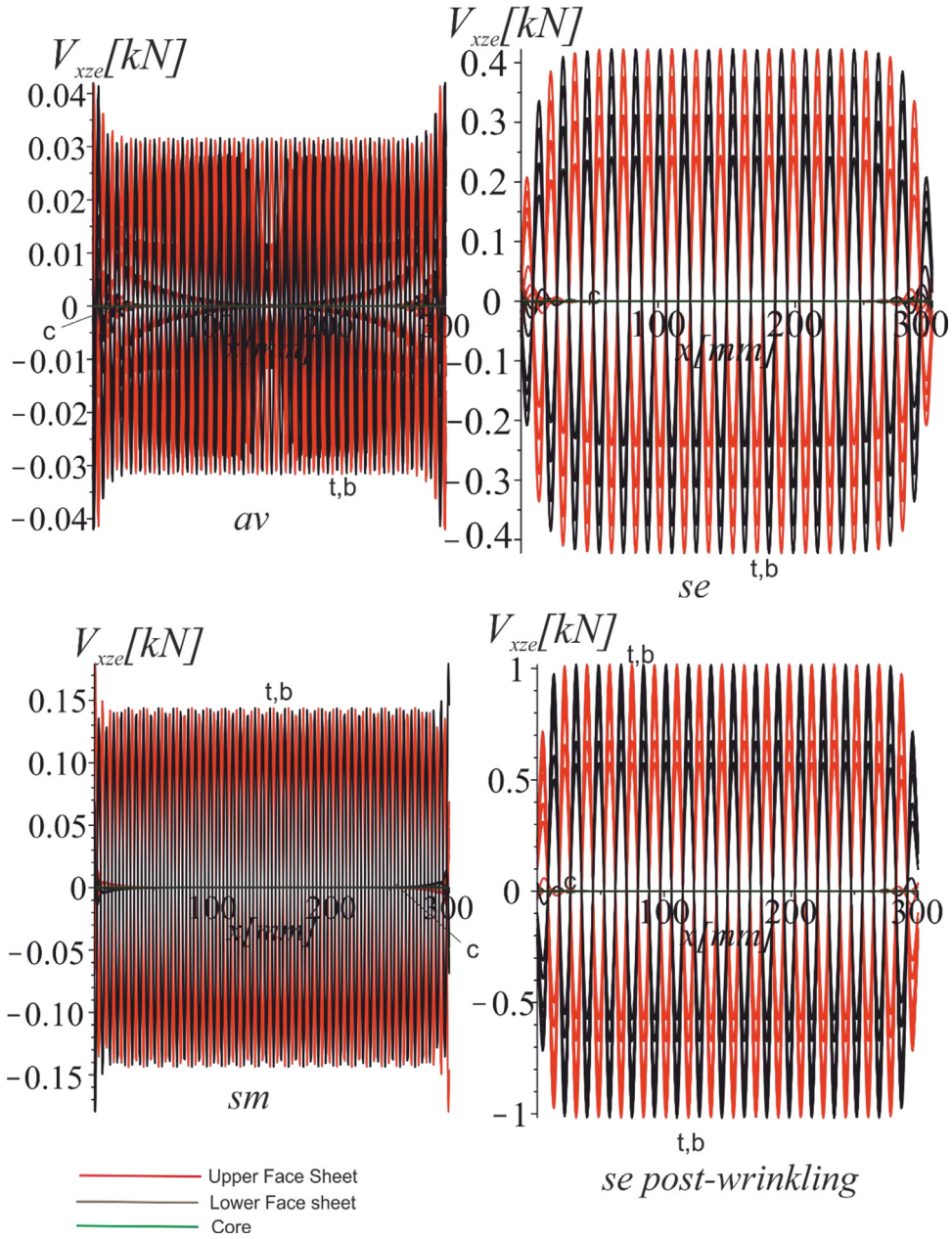


Fig. 8. Transverse shear forces upon wrinkling along the span of the sandwich panel subject to controlled displacement.

$$\begin{aligned}
 N_{xxeb}(x) &= N_{xxb}(x) + 4 \frac{M_{xx3c}(x)}{c^3} + 2 \frac{M_{xx2c}(x)}{c^2} \\
 M_{xxeb}(x) &= -M_{xxb}(x) + 2 \frac{M_{xx3c}(x)d_b}{c^3} + \frac{M_{xx2c}(x)d_b}{c^2} \\
 V_{xzeb}(x) &= \\
 & - \left(\frac{d}{dx} M_{xx2c}(x) \right) d_b c - 2 \left(\frac{d}{dx} M_{xx3c}(x) \right) d_b + \left(\frac{d}{dx} M_{xxb}(x) \right) c^3 + \\
 & \frac{N_{xxb}(x) \left(\frac{d}{dx} w_b(x) \right) c^3 + c(c + 2d_b) M_{xz1c}(x) + (2c + 6d_b) M_{xz2c}(x) - m_b(x) c^3}{c^3} \\
 N_{xxec}(x) &= N_{xxc}(x) - 4 \frac{M_{xx2c}(x)}{c^2} \\
 M_{xxec}(x) &= \frac{M_{xxc}(x) - 4M_{xx3c}(x)}{c^2} \\
 V_{xzec}(x) &= Q_{xzc}(x) - 4 \frac{M_{xz2c}(x)}{c^2}
 \end{aligned} \tag{11}$$

Note that compared to the formulation in Frostig (2011), the use of the equivalent stress resultants yields relatively simple equilibrium equations and boundary conditions that are defined in terms of the equivalent quantities only.

The stress resultants and couples in the core, including both conventional and higher-order contributions are defined by

$$\begin{aligned}
 [N_{xxc}, M_{xxc}, M_{xx1c}, M_{xx2c}] &= \int_{-\frac{1}{2}c}^{\frac{1}{2}c} \{1, z_c, z_c^2, z_c^3\} b_w \sigma_{xx}(x, z_c) dz_c \\
 [Q_{xzc}, M_{xz1c}, M_{xz2c}] &= \int_{-\frac{1}{2}c}^{\frac{1}{2}c} \{1, z_c, z_c^2\} b_w \tau_{xz}(x, z_c) dz_c \\
 [R_{zzc}, M_{zzc}] &= \int_{-\frac{1}{2}c}^{\frac{1}{2}c} \{1, z_c\} b_w \sigma_{zz}(x, z_c) dz_c
 \end{aligned} \tag{12}$$

where b_w is the width of the panel.

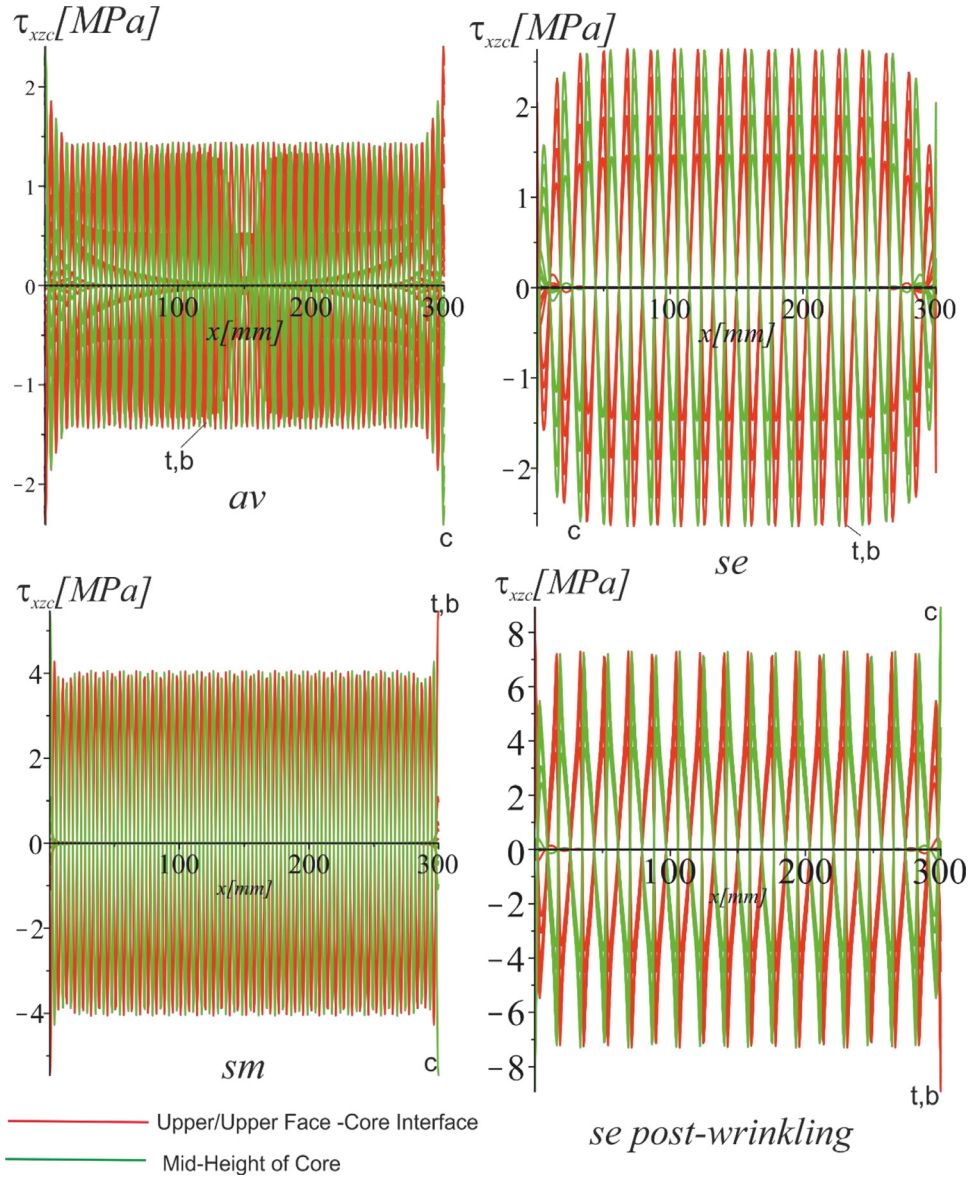


Fig. 9. Transverse shear stresses in the core upon wrinkling along the span of the sandwich panel when subject to controlled displacement.

The mechanical properties of the FGM core are introduced through the moduli of elasticity of the core in the longitudinal and vertical directions that are dependent on the vertical (z) coordinate, $E_{cx}(x, z_c)$ and $E_{cz}(x, z_c)$, respectively, and the shear modulus $G_{xzc}(x, z_c)$. A specific distribution of these properties is presented in the numerical study section. The conventional core scenario is recovered from the FGM formulation by assuming that all above moduli are independent of the vertical coordinate.

The stress and the displacements fields in the core are required in order to explicitly present field Eq. (10). They are determined using the core strains, Eq. (7), and the FGM core properties. The

core stress fields read:

$$\sigma_{xxc}(x, z_c) = \frac{E_{cx}(x, z_c) \left(\begin{aligned} & d_b z_c^2 (c + 2z_c) \frac{d^2}{dx^2} w_b(x) - d_t z_c^2 (c - 2z_c) \frac{d^2}{dx^2} w_t(x) + \\ & 2z_c^2 (c + 2z_c) \frac{d}{dx} u_{ob}(x) + 2z_c^2 (c - 2z_c) \frac{d}{dx} u_{ot}(x) + \\ & c \left((c^2 z_c - 4z_c^3) \frac{d}{dx} u_1(x) + (c^2 - 4z_c^2) \frac{d}{dx} u_0(x) + \right. \end{aligned} \right)}{c^3 (\mu_{xz} \mu_{zx} - 1)}$$

$$\sigma_{zxc}(x, z_c) = \frac{E_{cz}(x, z_c) \left(\begin{aligned} & d_b z_c^2 \mu_{xz} (c + 2z_c) \frac{d^2}{dx^2} w_b(x) - d_t z_c^2 \mu_{xz} (c - 2z_c) \frac{d^2}{dx^2} w_t(x) + \\ & 2z_c^2 \mu_{xz} (c + 2z_c) \frac{d}{dx} u_{ob}(x) + 2z_c^2 \mu_{xz} (c - 2z_c) \frac{d}{dx} u_{ot}(x) + \\ & c \left((c^2 \mu_{xz} z_c - 4 \mu_{xz} z_c^3) \frac{d}{dx} u_1(x) + (c^2 \mu_{xz} - 4 \mu_{xz} z_c^2) \frac{d}{dx} u_0(x) + \right. \end{aligned} \right)}{c^3 (\mu_{xz} \mu_{zx} - 1)}$$

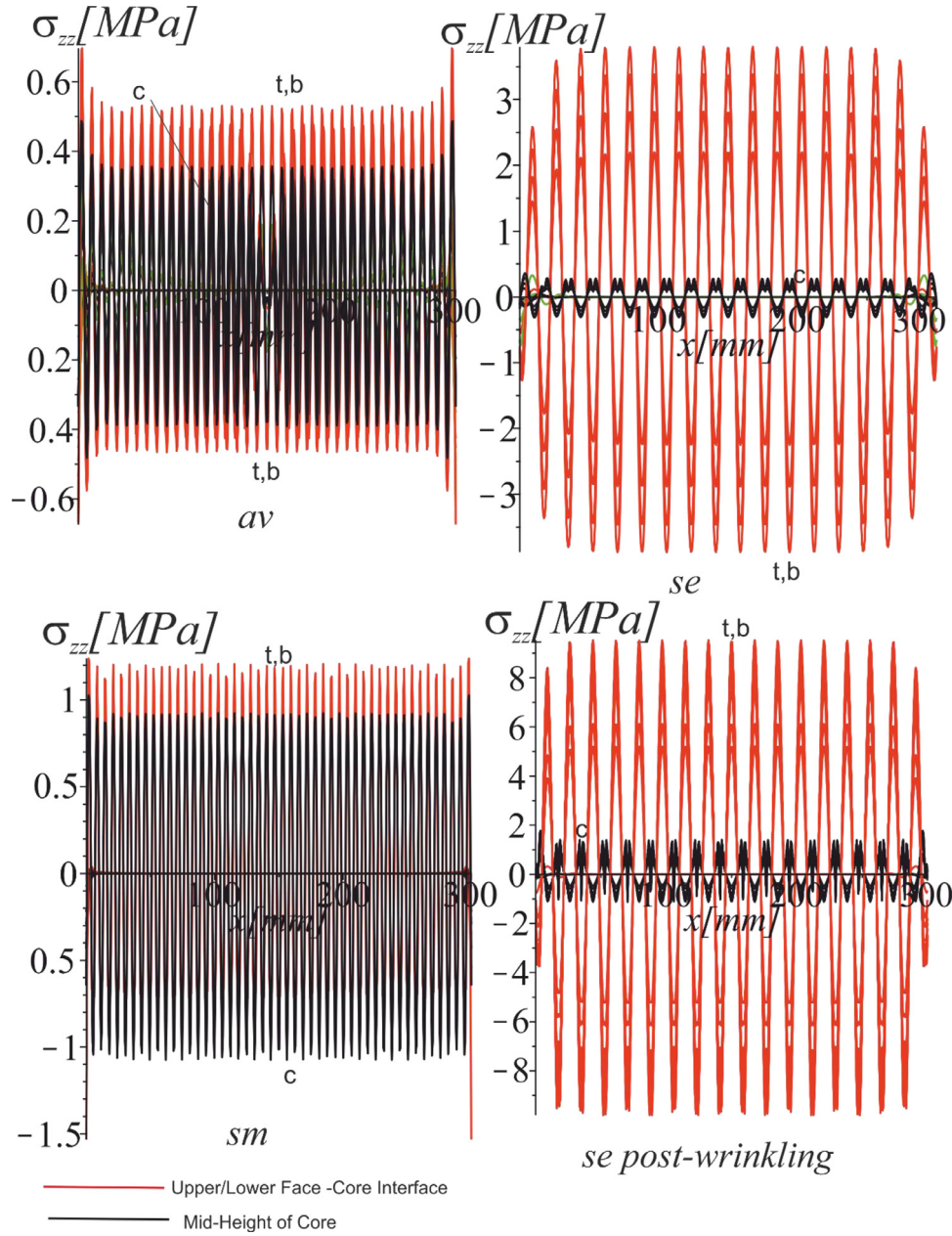


Fig. 10. Interfacial normal stresses upon wrinkling along the span of the sandwich panel when subject to controlled displacement.

$$\tau_{xz}(x, z_c) = \left(\begin{array}{l} ((2c + 6d_b)z_c + c(c + 2d_b))z_c \frac{d}{dx} w_b(x) - \\ ((-2c - 6d_t)z_c + c(c + 2d_t))z_c \frac{d}{dx} w_t(x) + \\ (c^3 - 4cz_c^2) \frac{d}{dx} w_o(x) + 4z_c(3z_c + c)u_{ob}(x) + \\ 4z_c(c - 3z_c)u_{\alpha}(x) + ((c^2 - 12z_c^2)u_1(x) - 8z_c u_o(x))c \end{array} \right) \frac{1}{c^3} G_{xz}(x, z_c) \quad (13)$$

where μ_{xz} and μ_{zx} are the Poisson ratios of the core that satisfy the following relation: $\mu_{xz}E_{cx} = \mu_{zx}E_{cz}$.

In addition, the boundary conditions obtained from the variational principle and shown below in terms of the equivalent quantities and displacements in the face sheets ($j=t,b$) and in the core

read

$$\begin{array}{ll} N_{xxej}(x_e)\alpha - N_{ej} = 0 & \text{or } u_{oj}(x_e) - u_{oej}(x_e) = 0 \\ -M_{ej} - \alpha M_{xxej}(x_e) = 0 & \text{or } D(w_j)(x_e) - D(w_{ej})(x_e) = 0 \\ V_{xzej}(x_e)\alpha - P_{ej} = 0 & \text{or } w_j(x_e) - w_{ej}(x_e) = 0 \\ N_{xxce}(x_e)\alpha - N_{ec} = 0 & \text{or } u_o(x_e) - u_{oec}(x_e) = 0 \\ M_{xxce}(x_e)\alpha - M_{ec} = 0 & \text{or } u_1(x_e) - Dw_{ec}(x_e) = 0 \\ V_{xzce}(x_e)\alpha - P_{ec} = 0 & \text{or } w_o(x_e) - w_{ec}(x_e) = 0 \end{array} \quad (14)$$

where N_{xxej} , V_{xzej} , and M_{xxej} ($j=t,b,c$) are the equivalent in-plane stress resultants, transverse shear stress resultants and bending stress couples, respectively, introduced in Eq. (11); N_{ej} , P_{ej} , and M_{ej} ($j=t,b,c$) are the external longitudinal and vertical load intensities and external bending stress resultant applied at the face sheets and at the core at the boundary $x=x_e$, u_{oej} , w_{ej} , and Dw_{ej} ($j=t,b,c$) are the in-plane and vertical displacements and the rotations of the

centroids of the face sheets and the core, respectively, $\alpha = 1$ when $x=L$ and $\alpha = -1$ when $x=0$.

The displacement fields in the core are obtained by the substitution of Eq. (9) into Eq. (6):

$$u_c(x, z_c) = \frac{\left(z_c^2 d_b(2z_c + c) \frac{d}{dx} w_b(x) - z_c^2 d_t(-2z_c + c) \frac{d}{dx} w_t(x) + 2z_c^2(2z_c + c)u_{ob}(x) + (2z_c^2 u_{ot}(x) + c(u_o(x) + u_1(x)z_c)(2z_c + c))(-2z_c + c) \right)}{c^3} \quad (15)$$

$$w_c(x, z_c) = w_o(x) + \frac{(-w_t(x) + w_b(x))z_c}{c} + 2 \frac{(w_t(x) - 2w_o(x) + w_b(x))z^2}{c^2}$$

The governing equations are derived by the substitution of the force-displacement relations for the isotropic face sheets into the field Eq. (10), along with the high-order stress resultants in the core given by Eqs. (11) and (13). The force-displacements relations for the isotropic face sheets ($j = t, b$) read:

$$N_{xxj}(x) = \int \sigma_{xxj}(x, z_j) dA = EA_j \left(\frac{d}{dx} u_{oj}(x) + 1/2 \left(\frac{d}{dx} w_j(x) \right)^2 \right)$$

$$M_{xxj}(x) = \int \sigma_{xxj}(x, z_j) z_j dA = -EI_j \frac{d^2}{dx^2} w_j(x) \quad (16)$$

where EA_j and EI_j ($j = t, b$) are the axial and the flexural rigidity of unit-width of each face sheet, respectively. Note that through Eq. (16) we formulate the problem in terms of forces and moments in a sandwich beam, rather than stress resultants and couples.

The resulting set of the 18 ordinary non-linear differential governing equations is derived through substitution of the stress resultant relations, Eqs. (11)–(13) into Eq. (10) using Maple (see Char et al., 1991). However the equations are very long and are omitted for brevity. Note that deformations of each constituent of the panel are defined through three unknowns, i.e. in-plane and vertical displacements and rotation of its centroid. The solution has been obtained numerically using a finite-difference approach that is implemented in the ODE solver of Maple, see Char et al. (1991). It uses trapezoid or mid-point methods with Richardson extrapolation or deferred corrections, (Ascher and Petzold, 1998), along with parametric or arc-length continuation methods (Keller, 1992).

3. Numerical study

The numerical study investigates the effects of the load transfer mechanism when the compressive external load is applied through the core's edge while the edges of the face sheets are free of any traction and when a prescribed axial displacement is uniformly applied both to the core and the face sheets through a rigid edge beam, see Fig. 2. In particular, we are interested in the effect of various distributions of FGM mechanical properties on the wrinkling response of the sandwich panel. The case where the load is applied through the core only can be addressed as "controlled force" since the magnitude of the applied force is known. In this case, the load is applied to the core through a rigid beam and re-distributed to the face sheets through the core close to the loaded edge. The case where uniform displacements are applied (uniform end shortening) at the edge of the sandwich panel may be called "controlled displacements." In this case, the external load is distributed based on the stiffness of the face sheets and the core at the linear and non-linear regime of response. Both cases are feasible in practical applications since the relevant joints can be designed and manufactured. In the case of controlled force, a rigid

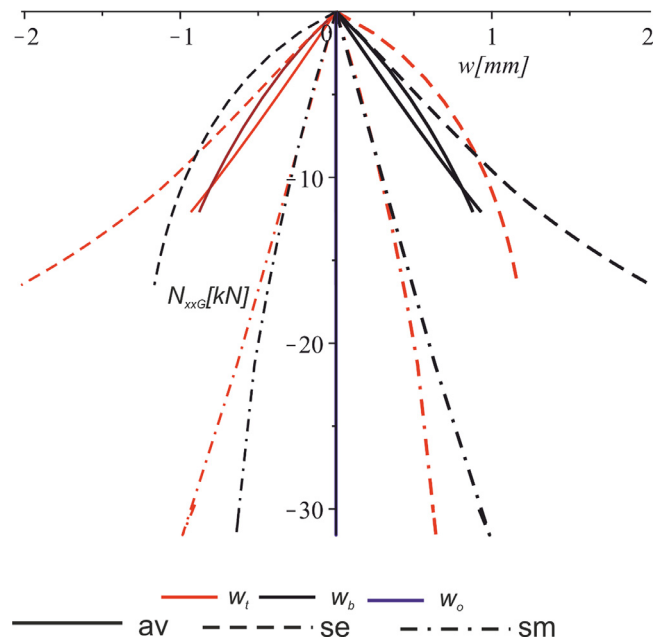


Fig. 11. Extreme vertical displacement as a function of the compressive controlled force at the edge $x=0$.

edge beam is extended through the depth of the core. In the joint designed for controlled displacements, a rigid edge beam extends throughout the entire depth of the sandwich panel. Note that in the first case (controlled force), the load should be symmetric about the middle plane of the panel, avoiding eccentricities. In the case of controlled displacements the rigid edge beam remains perpendicular to the middle plane of the panel, producing symmetric loading on the identical face sheets and in the core.

The sandwich panel considered in numerical analysis had the width of 60 mm and the length of 300 mm. The face sheets are 0.5 mm thick and the core thickness is 19.05 mm. The identical Kevlar/epoxy laminated composite face sheets has an equivalent modulus of elasticity of 27,400 MPa. The isotropic core is made of Rohacell where its elasticity and shear moduli varies in the vertical direction. Geometry, boundary conditions, load transfer and FGM properties distributions are depicted in Fig. 2. In order to achieve a non-trivial (out of plane) wrinkling solution, a small distributed load $q_{zt} = -q_{zb} = 0.001 \text{ N/mm}$ is applied to the face sheets.

The study examines two types of symmetric property distributions through the depth of the core, as reflected in Fig. 2b. The first case where the stiffer core properties are at the face core interface is denoted by "se", while the second case is where the material is relatively compliant at the core interfaces and stiffer at the mid-height of core is denoted by "sm". The case of a homogeneous core with uniform through-the-thickness properties is denoted by "av". The stiffness corresponding to this case corresponds to the average of the se case. Note that the average of the sm case properties is larger than those of the homogeneous av case, so it can be anticipated that the former panel will be heavier.

The FGM distribution depends on the distribution of the density of the material through the depth of the core. The moduli increase in denser core and decrease in the core with a low density. The moduli-density relationships adopted here were developed for foam materials (Gibson and Ashby, 1997):

$$E_c(\rho_c) = k_1 \left(\frac{\rho_c}{\rho} \right) (z_c)^{n_1} E, \quad G_c(\rho_c) = k_2 \left(\frac{\rho_c}{\rho} \right) (z_c)^{n_2} G$$

where E and G are moduli of solid foam material, k_1, k_2, n_1 and n_2 are material constants and ρ_c and ρ are foam and solid foam

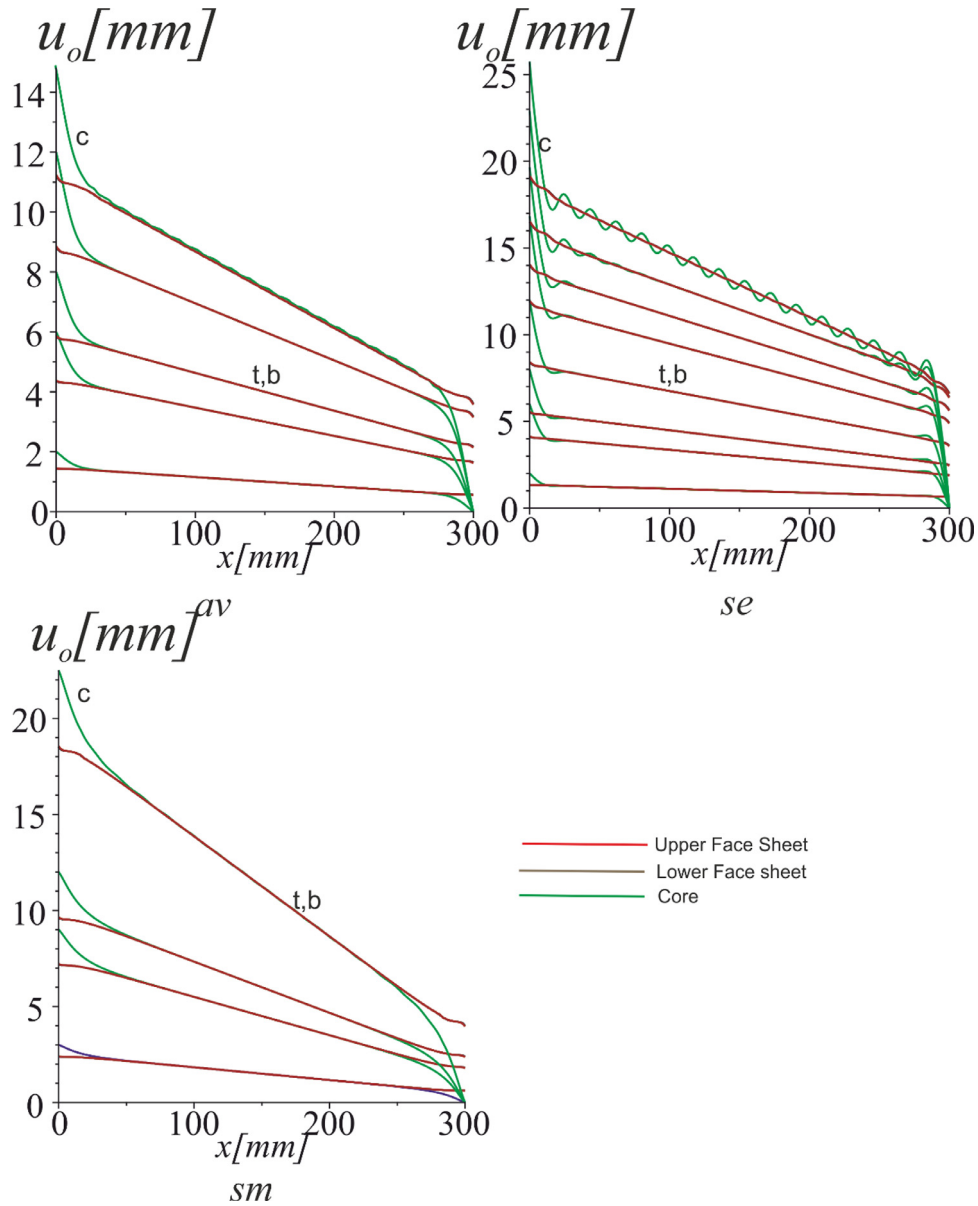


Fig. 12. Longitudinal displacements along the middle plane of the panel prior to and after wrinkling under controlled compressive force applied at the left end ($x=0$).

material densities, respectively. For the particular case considered here, these values are: $E=905.8$ MPa, $G=370.4$ MPa. $k_1=1$, $k_2=0.4$, $n_1=2$, $n_2=2$.

For a symmetric core material distribution the variation of the density ratio through the thickness is described by a parabola:

$\frac{\rho_c}{\rho}(z_c) = a_1 z_c^2 + a_0$, with the limiting conditions for the *se* case where $\frac{\rho_c}{\rho}(z_c=0) = 0.05$ and $\frac{\rho_c}{\rho}(z_c=c/2) = 0.5$. For the *sm* case, these conditions were inverted. Hence, the mechanical properties are:

a. Stiffer core at the face-core interfaces (*se*):

$$E_c(z_c) = 905.7971014 \left(1.80 \frac{z_c^2}{c^2} + 0.050 \right)^2,$$

$$G_c(z_c) = 370.4433498 \left(1.80 \frac{z_c^2}{c^2} + 0.050 \right)^2$$

b. The homogeneous core with the average through-the-thickness properties, (*av*):

$$E_c(z_c) = 52.5 \text{ MPa}, \quad G_c(z_c) = 21.0 \text{ MPa}$$

c. Stiffer core at the middle plane (*sm*):

$$E_c(z_c) = 905.7971014 \left(-1.80 \frac{z_c^2}{c^2} + 0.500 \right)^2, \quad G_c(z_c) = 370.4433498 \left(-1.80 \frac{z_c^2}{c^2} + 0.500 \right)^2$$

As noted above, the average properties of the *sm* case are larger than their counterparts in the case *av*.

Two cases of load transfer mechanism have been studied. In one case the compressive load is applied to both the face sheets and the core through a rigid edge beam that yields a uniform end-shortening for all sandwich components (controlled displacements). In this case both the face sheets and the core are simply-supported at the edges. In the other case the compressive load is applied through a rigid edge beam to the edges of the core only, while the core is simply-supported and the face sheets are free at the edges. In the controlled displacement case the in-plane displacements of the centroid of each face sheets and core displace-

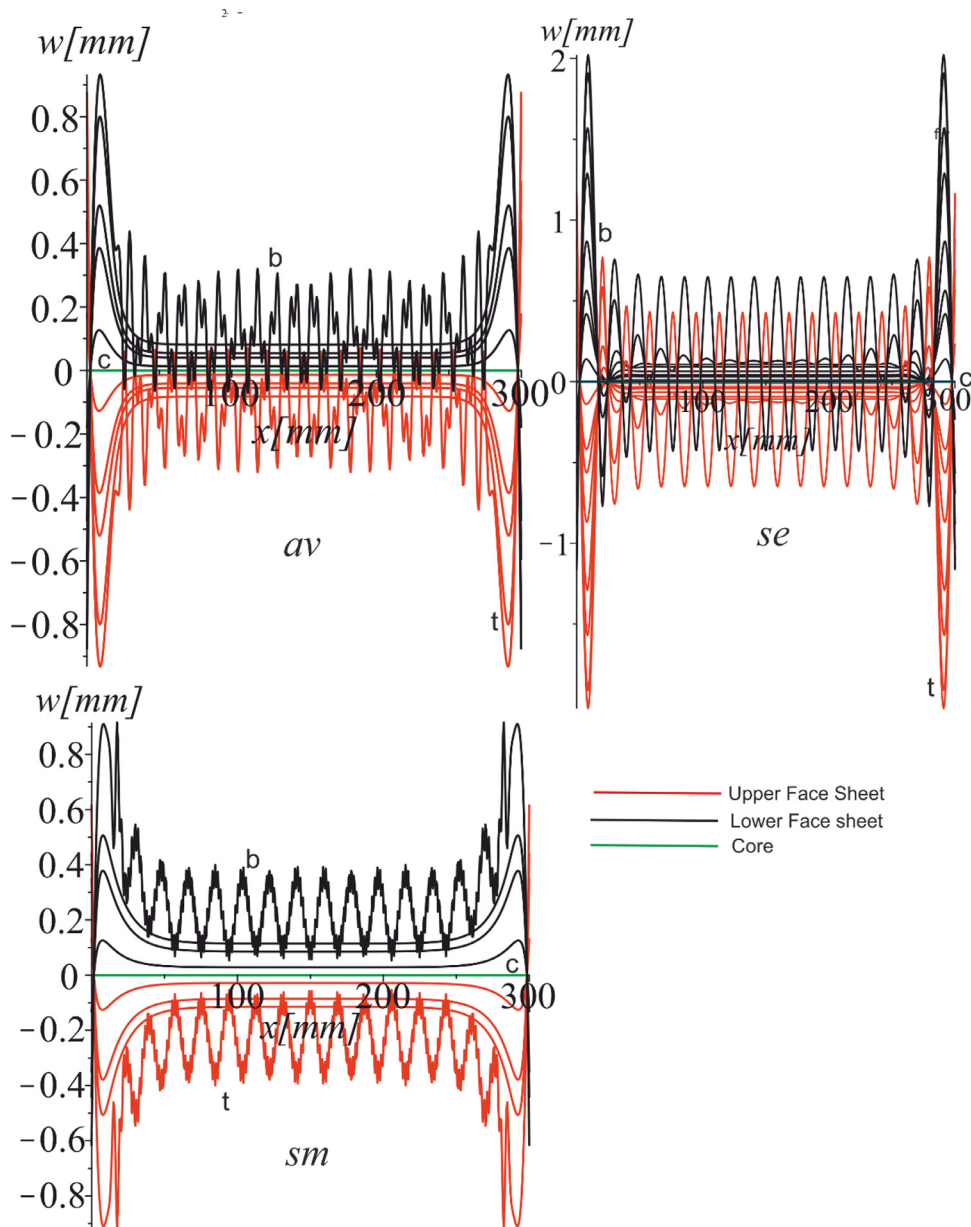


Fig. 13. Vertical displacements of the top and lower facings along the span of the sandwich panel when subject to controlled force.

ments are identical within the linear response range. The compressive loads in the case of controlled displacement are introduced through a change in the longitudinal displacement of the loaded edge.

The following results concentrate on wrinkling of the panels subject to the controlled displacements or forces. To get a better insight into the post-wrinkling nonlinear behavior, the post-wrinkling results are also demonstrated for functionally graded core panels with a higher stiffness near the interfaces with the facings (case *se*).

Problem 1: Wrinkling under controlled axial displacements

The extreme vertical (out-of-plane) displacement is shown as a function of the compressive force generated by a controlled compressive displacement in Fig. 3. In all cases the displacements increase linearly with the axial force, prior to wrinkling. This reflects a uniform increase of the thickness of the panel undergoing controlled compressive displacements at the edge $x=0$ while the opposite edge is restrained. The changes in the slope of the equi-

librium curves reveal the onset of wrinkling. They occur at the force N_{xxG} of an order of 10 kN in the panel with a homogeneous core and between 14 kN and 16 kN in the panels with functionally graded cores. The increase in the wrinkling axial force in functionally graded panels in case *se* as compared to the homogeneous core *av* is understandable since stiffer sections of the core provide additional support to the face sheets. In case *sm* such increase may seem counterintuitive since the stiffness of the core adjacent to the face sheets is reduced as compared to cases *av* and *se*. However, the overall stiffening of the core achieved at the expense of a larger weight explains the large wrinkling resistance of panels *sm*. The secondary branches observed in functionally graded panels reveal the presence of a buckling point in the panels with a functionally graded core that is absent in the panel with a homogeneous core.

The conclusions from Fig. 4 demonstrating a relationship between the maximum longitudinal controlled displacement and the resulting compressive force are identical to those obtained from

Fig. 3. A sharp reduction in the stiffness reflected in a large reduction in the force gradient is a symptom of wrinkling.

As follows from Fig. 5, longitudinal displacements vary linearly prior to wrinkling from the loaded to the restrained end of the panel in both homogeneous *av* and functionally graded core cases (*se* and *sm*). However, upon wrinkling short wrinkling waves are superimposed on the straight line between the maximum displacement at the loaded end $x=0$ and the opposite restrained end as is shown for case *se*. The presence of these superimposed waves reflects the onset of wrinkling at the controlled longitudinal displacement of about 10 mm and the subsequent post-wrinkling nonlinear behavior. The controlled displacements shown for cases *av* and *sm* did not reach the wrinkling stage; accordingly, superimposed wrinkling waves are not shown in the corresponding graphs.

The pattern of wrinkling is similar for both homogeneous and functionally graded core panels as demonstrated in Fig. 6. The amplitudes of short wrinkles are nearly identical over the span of the panel, except for the narrow regions adjacent to the edges. In the panels with a functionally graded core that is stiffer adjacent to the face sheets *se* the wrinkles are noticeably smaller near the edges. The situation is reversed in panels with a stiffer core at the middle plane *sm*. The difference between the amplitudes in the three cases considered here is related to different magnitudes of controlled axial displacements. In addition to the pattern of wrinkles at the wrinkling controlled displacement shown for all three core cases, the post-wrinkling pattern is demonstrated in case *se*. While the wrinkle amplitudes increase, the pattern of waves remains unchanged in the post-wrinkling phase. Smaller amplitudes in a functionally graded core panel with a higher stiffness at the middle plane *sm* as compared to case *se* are related to the higher average overall stiffness of the core.

The distribution of bending moments upon wrinkling (cases *av* and *sm*) and both upon wrinkling and in the nonlinear post-wrinkling state (case *se*) are shown in Fig. 7. In the panels with a homogeneous core the moments with larger amplitudes are adjacent to the edges. The situation is reversed in panels with a functionally graded core that is stiffer near the facings *se*. In panels with a stiffer graded core at the middle plane (*sm*) the amplitude remains nearly constant throughout the span. In the post-wrinkling phase the amplitudes of the moment change, but the pattern of its distribution is not altered (*se*).

A comparison of the transverse shear forces in Fig. 8 reflects a higher support of the facings by both functionally graded cores. In both functionally graded cores the controlled wrinkling longitudinal displacement is larger than in the homogeneous core, explaining larger post-wrinkling forces. Three-dimensional effects are clearly observed in the vicinity to the edges in all cases considered, though they produce different outcomes, the most noticeable being lower amplitude near edges values compared to the amplitudes in the central section of the span in case *se*. Post-wrinkling nonlinear response shown for the case *se* does not alter the pattern of the force distribution over the span, though the amplitude increase.

The distribution of transverse shear stresses in the core is shown in Fig. 9. Three-dimensional effects in the vicinity to the edges result in a higher stress amplitude in this area compared to amplitudes within the rest of the span in the cases of a homogeneous core and, to a lesser extent, in a functionally graded core with a higher stiffness at the middle plane (cases *av* and *sm*, respectively). In the functionally graded panel with stiffer core adjacent to the face sheets, (case *se*), transverse shear stresses have a smaller amplitude near the edges. The largest stresses in both functionally graded panels exceed those in the panel with a homogeneous core. This is a consequence of a stiffer core adjacent to the face sheets (case *se*) and a larger average core stiffness (case *sm*). The trends observed for wrinkling response are not altered in the post-wrinkling phase as shown in case *se*.

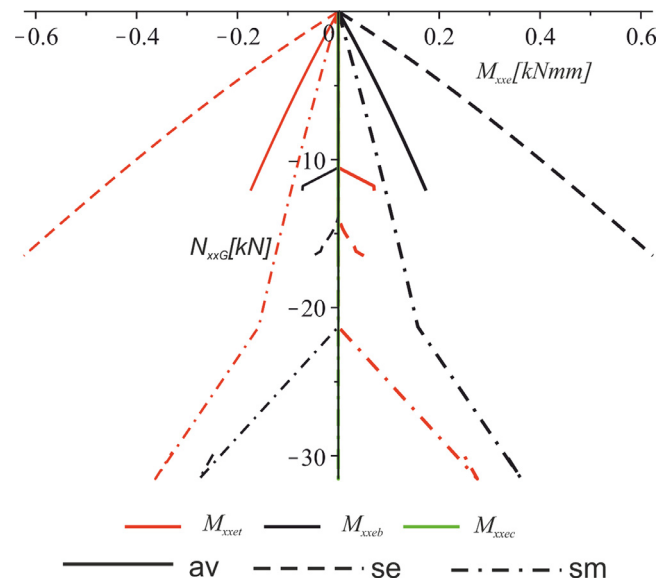


Fig. 14. Controlled axial force vs. equivalent bending moment at the face sheets and the core.

The observations regarding the distribution of transverse shear stresses remain valid for facing-core interfacial normal stresses as shown in Fig. 10. The magnitude of these stresses in the cases of a homogeneous core or a core that is stiffer near the middle plane is smaller than the transverse shear counterparts upon wrinkling as well as in the post-wrinkling phase complying with well-documented knowledge. However, the relationship between the transverse shear and normal stresses can change in the nonlinear post-wrinkling phase (compare case *se*: post-wrinkling in Figs. 9 and 10). Based on the results in Figs. 9 and 10, it is possible to conclude that the core failure will likely originate at the edges in the homogeneous core and in the graded core that is stiffer at the middle plane, while in the core of the panel with a stiffer core adjacent to the facing failure will originate within the span.

Problem 2: Wrinkling under controlled axial force

Wrinkling under controlled compressive force is generally similar to wrinkling under controlled axial displacement. However, there are differences in the response due to different edge joints. Accordingly, only selected representative results are presented in this section.

The extreme vertical displacement is demonstrated as a function of the compressive controlled force in Fig. 11. Nonlinearity is exhibited under this type loading, particularly noticeable in case *se*, even at relatively small values of the force. At first, this phenomenon is puzzling, but as follows from the following figures, it can easily be explained by formation of a single deformation half-wave at the edges even at low load.

The axial displacement distribution along the middle plane of the core throughout the span is demonstrated in Fig. 12. Even prior to wrinkling, three-dimensional effects are clearly indicated at the edges of the panel reflecting single half-waves of the deformation facilitated by the local shear lag phenomenon between the face sheets and core. Such phenomenon that was not observed in the case of controlled displacement reflects the observation that extreme vertical displacements in Fig. 11 do not adequately predict wrinkling since they refer to the local deformations at the edges, even while the major part of the span does not wrinkle. These observations about the sequence of deformation and wrinkling under loading are confirmed by the results in Fig. 13 showing the distribution of vertical displacements throughout the span of the panel.

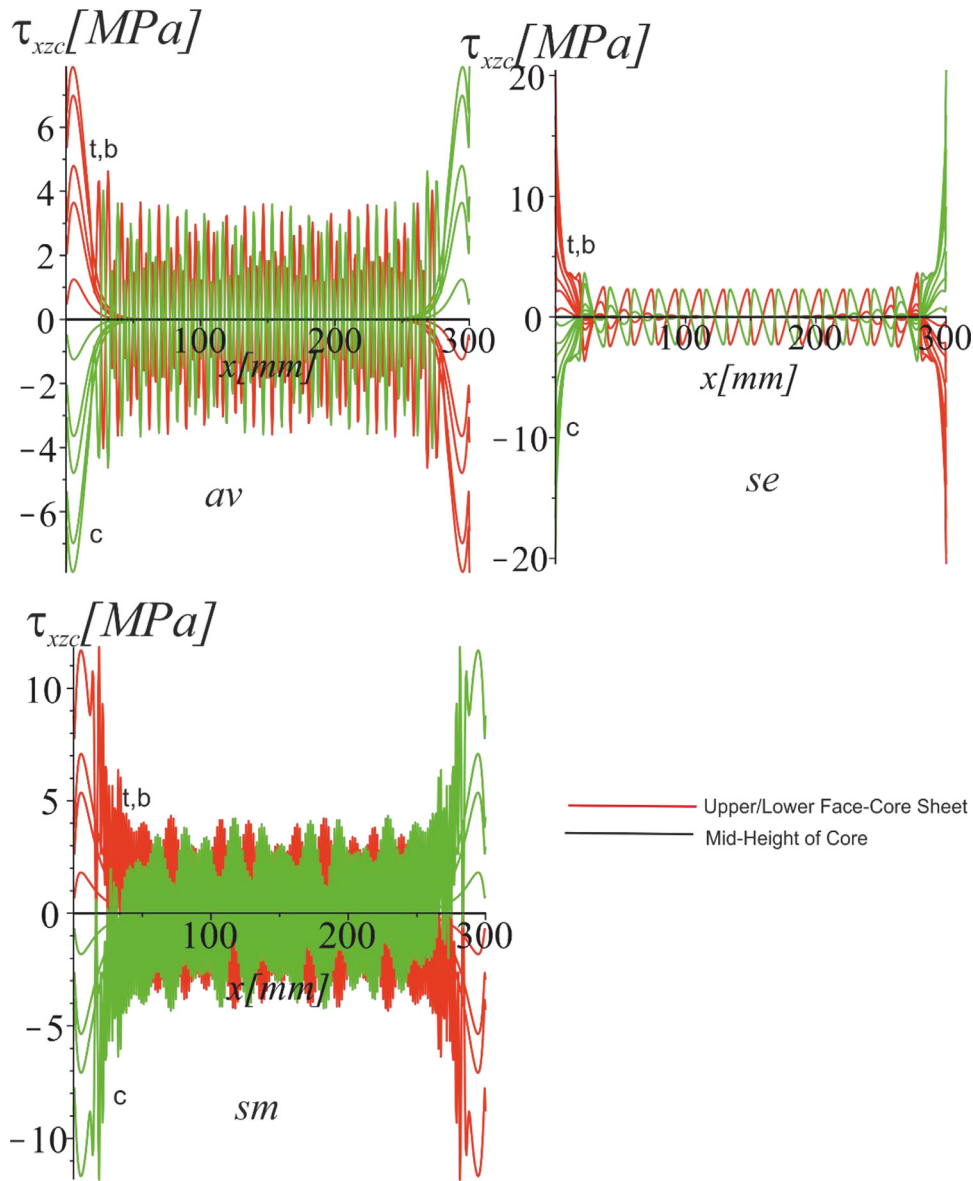


Fig. 15. Transverse shear stresses in the core upon wrinkling under controlled force.

A single half-wave of deformation adjacent to the edges prior to overall wrinkling is clearly observed in this figure.

Because of local waves developing adjacent to the edges due to the three-dimensional effect even at a low controlled force, the wrinkling force resulting in wrinkling over the entire span is rather difficult to detect from Figs. 11 and 12. However, this force is determined from Fig. 14 showing the variation of the equivalent bending moment in the facings and core as a function of the applied controlled force. The secondary branches of the corresponding curves indicate the load resulting in the overall wrinkling. Accordingly, the wrinkling force is about 11 kN, 15 kN and over 20 kN in cases *av*, *se* and *sm*, respectively. The fact that the wrinkling force is higher in the graded core that is stiffer at the middle plane is reasonable in the controlled force type of loading where the force is applied to the core directly and redistributed to the stiff facings. This represents a major difference from the case of controlled displacements where the axial displacement in the facings and core is kept identical prior to wrinkling. The equivalent moment remains equal to zero at the middle plane of the core

throughout the loading process meaning that wrinkling is symmetric about the middle plane.

A distribution of transverse shear stress in the core (Fig. 15) and interfacial normal stress throughout the length of the span (Fig. 16) is also instructive. Contrary to the case of controlled displacements, the peak stresses occurring at the edges of the panel significantly exceed the corresponding stress amplitudes in the span in all three cases reflecting shear lag phenomenon and are a result of the load transfer mechanism from the core to the edges, see Fig. 15.

Finally, the pattern of progressive deformation is shown for wrinkling under controlled force and controlled displacement in Figs. 17 and 18, respectively. The shapes of sandwich panels shown in these figures confirm our observations above, i.e. a significant three-dimensional effect is observed in panels with a stiffer core in the vicinity to the facings undergoing controlled force. Such local deformations can cause failure prior to the loss of strength of the core or face sheets in the sections adjacent to the edges or delamination of the core from the face sheets prior to wrinkling. This demonstrates the necessity of considering all possible modes

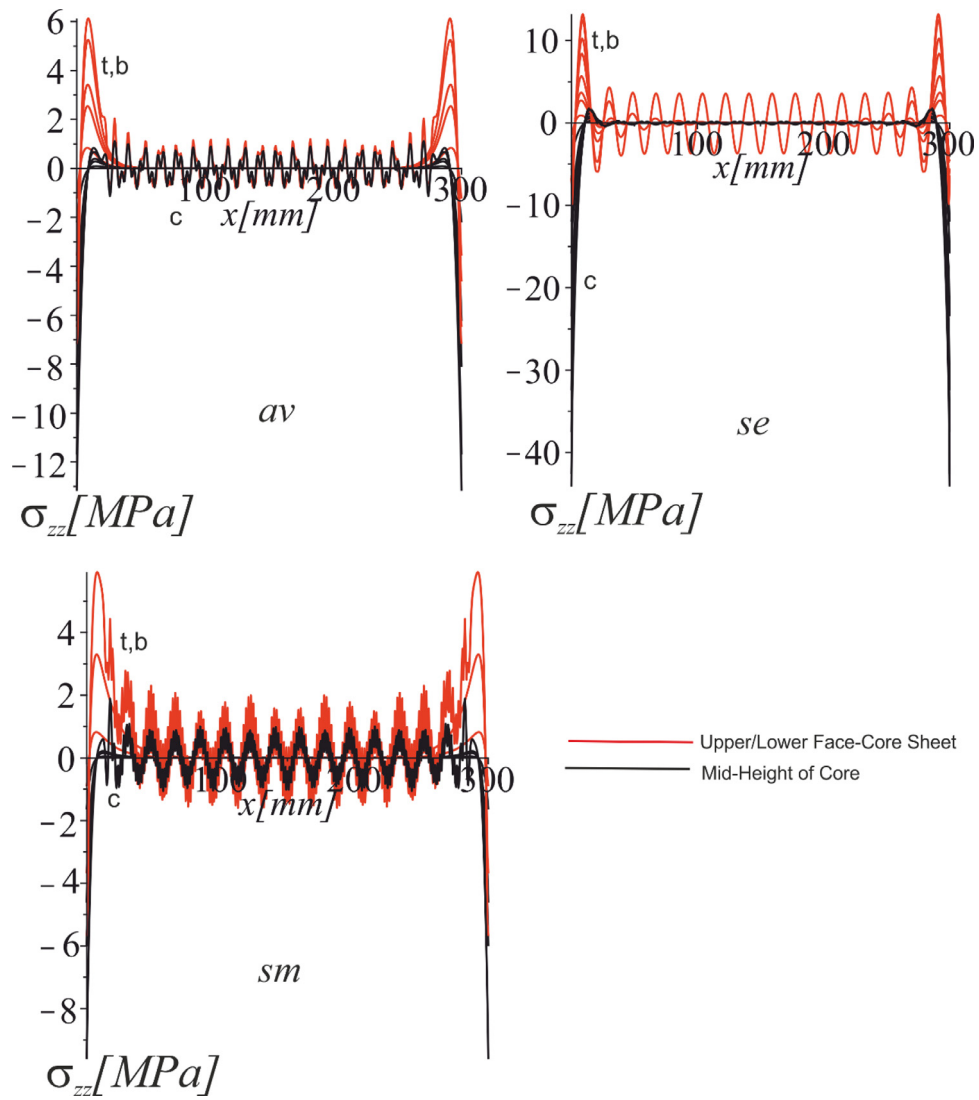


Fig. 16. Interfacial normal stresses upon wrinkling under controlled force.

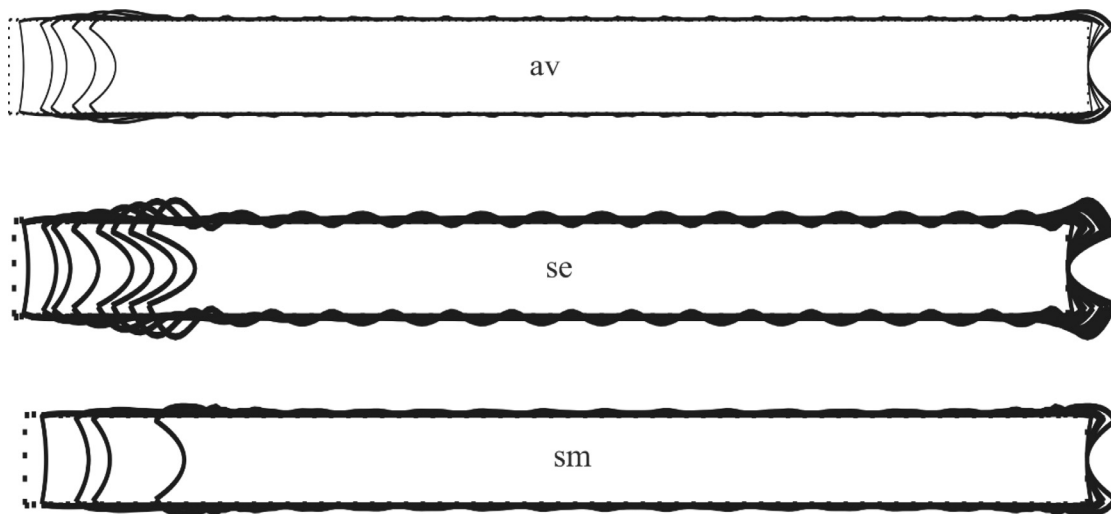


Fig. 17. Deformed shapes of a progressively loaded panel when subject to controlled force.

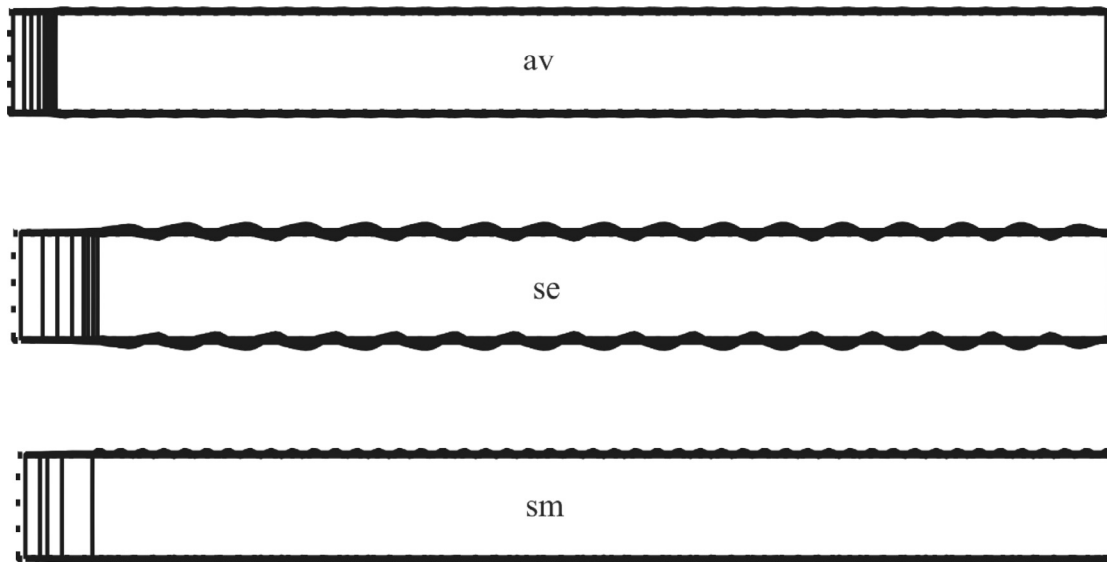


Fig. 18. Deformed Shapes of a progressively deformed panel subject to controlled displacement (uniform end shortening).

of failure designing composite and sandwich structures and a careful analysis of their joints.

4. Summary and conclusions

The High-Order Sandwich Panel Theory is extended to analyze wrinkling instability and post-wrinkling behavior of sandwich panels with a functionally graded core. The goals of the analysis include:

- Investigation whether functional grading of the core can increase wrinkling axial controlled displacements or wrinkling forces, without the penalty of a higher weight of the structure;
- Comparison of the response and efficiency of grading schemes dependent on different loading scenarios (and different joint designs), namely controlled displacement and controlled force;
- Examination whether geometric nonlinearities affecting post-wrinkling response alter the pattern of wrinkles;
- Suggestion of a preferable grading for the core.

The study addresses all goals listed above and resulted in the following conclusions and observations.

A functionally graded core can improve wrinkling stability of sandwich structures. In particular, employing higher stiffness adjacent to the face sheets may increase the axial controlled wrinkling displacement without a detrimental effect on the weight of the structure. Using a functionally graded core with stiffer sections at and in the vicinity of the middle plane may also be beneficial but at the expense of a larger weight. While a functionally graded core can improve wrinkling stability, the post-wrinkling stresses may actually increase compared to the case of a homogeneous core as a result of higher support against deflections of the face sheets.

Some tendencies that are not prominent in conventional composite structures may become essential in functionally graded counterparts. For example, a three-dimensional effect at the edges and associated local stresses can cause failure prior to the overall wrinkling. In addition, interfacial normal stresses may exceed transverse shear stresses in the panels with a functionally graded core. Post-wrinkling loading of the panel by either controlled displacement or controlled force does not qualitatively affect the pattern of deformation. Predictably, the stresses increase in the post-wrinkling phase, i.e. the ultimate failure of a wrinkled panel is the loss of strength.

While the advantages of using a functionally graded core have been demonstrated for both types of loading considered in the paper, there are pronounced differences in the response. In the case of controlled displacement where the prewrinkling displacements are uniform throughout the depth of the panel, wrinkling occurs simultaneously, at the same displacement, across the entire span. The situation is different in the panels subject to controlled force applied through the core and transmitted to the face sheets. In this case, three-dimensional effects near the edges predominate resulting in one half-wave of deformation adjacent to both edges of the panel even at low forces. Accordingly, the stresses at the edges are much higher than in the rest of the panel span. While wrinkling occurs throughout the span at certain loads, the mode of failure may actually be the loss of strength in the core adjacent to the edges due to the three-dimensional effect, prior to overall wrinkling along the span. This demonstrates the importance of the joint at the edges of sandwich structures loaded by axial displacement or force since the design of this joint may dictate both the failure load and the mode of the failure.

Acknowledgment

The financial support of the Office of Naval Research, USA, Grant N00014-16-1-2831, and the interest and encouragement of the Grant Monitor, Dr. Y.D.S. Rajapakse, are both gratefully acknowledged.

References

- Allen, H.G., 1969. *Analysis and Design of Structural Sandwich Panels*. Pergamon Press, London.
- Apetre, N.A., Sankar, B.V., Ambur, D.R., 2008. Analytical modeling of sandwich beams with functionally graded core. *J. Sandw. Struct. Mater.* 10, 53–74.
- Ascher, U.M., Petzold, L., 1998. *Computer Methods for Ordinary Differential Equations and Differential-Algebraic Equations*. SIAM, Philadelphia.
- Birman, V., 2014. In: Hetnarski, R.B. (Ed.), *Functionally Graded Materials and Structures*. *Encyclopedia of Thermal Stresses*. Springer, Dordrecht, pp. 1858–1864.
- Birman, V., Byrd, L.W., 2007. Modeling and analysis of functionally graded materials and structures. *Appl. Mech. Rev.* 60, 195–216.
- Birman, V., Keil, T., Hosder, S., 2012. In: Thomopoulos, S., Birman, V., Genin, G.M. (Eds.), *Functionally Graded Materials in Engineering*. *Structural Interfaces and Attachments in Biology*. Springer, New York, pp. 19–41.
- Birman, V., Vo, N., 2017. Wrinkling in sandwich structures with a functionally graded core. *J. Appl. Mech.* 81 pp. 021002-1 to 021002-8.

- Bozhevolnaya, E., Frostig, Y., 2006. Local effects at core junctions in sandwich beams – high-order modeling and experimental validation. *J. Aircr.* 43 (1), 189–193 Jan–Feb.
- Carrera, E., Brischetto, S., 2009. A survey with numerical assessment of classical and refined theories for the analysis of sandwich plates. *Appl. Mech. Rev.* 62 (1) 010803-1–010803-17.
- Char, B.W., Geddes, K.O., Gonnet, G.H., Leong, B.L., Monagan, M.B., Watt, S.M., 1991. *Maple V Library Reference Manual*. Springer, New-York.
- Dodds, R.H., Schwalbe, K.H., Paulino, G.H., 2002. *Fracture of Functionally Graded Materials*. Pergamon, New York.
- Frostig, Y., Baruch, M., Vilnai, O., Sheinman, I., 1992. High-order theory for sandwich-beam bending with transversely flexible core. *J. ASCE, EM Div.* 118 (5), 1026–1043.
- Frostig, Y., Kardomateas, G.A., Rodcheuy, N., 2016. Non-linear response of curved sandwich panels – extended high-order approach. *Int. J. Non-Linear Mech.* 81, 177–196.
- Frostig, Y., 2011. On wrinkling of a sandwich panel with a compliant core and self-equilibrated loads. *J. Sandw. Struct. Mater.* 13 (6), 663–679.
- Frostig, Y., Thomsen, O.T., 2009b. On the vibration of sandwich panels with a flexible and material temperature dependent core – part ii – numerical study. *Compos. Sci. Technol.* 69 (6), 863–869.
- Frostig, Y., Thomsen, O.T., 2009a. On the free vibration of sandwich panels with a flexible and material temperature dependent core – part i – mathematical formulation. *Compos. Sci. Technol.* 69 (6), 856–862.
- Frostig, Y., Thomsen, O.T., 2008. Thermal buckling and post-buckling of sandwich panels with a transversely flexible core. *AIAA J.* 46 (8), 1976–1989 Aug 2008.
- Frostig, Y., Thomsen, O.T., 2005. Localized effects in the non-linear behavior of sandwich panels with a transversely flexible core. *J. Sandw. Struct. Mater.* 7 (1), 53–75 Jan.
- Frostig, Y., Baruch, M., 1993. Buckling of simply-supported sandwich beams with transversely flexible core – a high order theory. *ASCE J. Eng. Mech.* 119, 955–972.
- Frostig, Y., Baruch, M., 1994. Free vibration of sandwich beams with a transversely flexible core: a high order approach. *J. Sound Vib.* 176 (2), 195–208.
- Genin, G.M., Kent, A., Birman, V., Wopenka, B., Pasteris, J.D., Marquez, P.J., Thomopoulos, S., 2009. Functional grading of mineral and collagen in the attachment of tendon to bone. *Biophys. J.* 97 (4), 976–985.
- Gibson, L.J., Ashby, M.F., 1997. *Cellular Solids, Structure and Properties*. Cambridge University Press, Cambridge.
- Kardomateas, G.A., 2005. Wrinkling of wide sandwich panels/beams with orthotropic phases by an elasticity approach. *J. Appl. Mech. (ASME)* 72, 818–825 Nov. 2005.
- Kardomateas, G.A., 2010. An elasticity solution for the global buckling of sandwich beams/wide panels with orthotropic phases. *J. Appl. Mech. (ASME)* 77 (2), 021015 (7 pages), March 2010.
- Kardomateas, G.A., Frostig, Y., Phan, C.N., 2013. Dynamic elasticity solution for the transient blast response of sandwich beams/wide plates. *AIAA J.* 51 (2), 485–491. doi:10.2514/1.J051885.
- Kardomateas, G.A., Phan, C.N., 2011. Three dimensional elasticity solution for sandwich beams/wide plates with orthotropic phases: the negative discriminant case. *J. Sandw. Struct. Mater.* 13 (6), 641–661. doi:10.1177/1099636211419127, November 2011.
- Keller, H.B., 1992. *Numerical Methods for Two-Point Boundary Value Problems*. Dover Publications, New York.
- Koizumi, M., 1997. FGM activities in Japan. *Compos. Part B Eng.* 28 (1–2), 1–4.
- Mindlin, R.D., 1951. Influence of rotatory inertia and shear on flexural motions of isotropic, elastic plates. *ASME J. Appl. Mech.* 18, 31–38.
- Miyamoto, Y., 1999. *Functionally Graded Materials: Design, Processing and Applications*. Kluwer Academic Publishers, Boston.
- Paulino, G.H., 2008. Multiscale and functionally graded materials. In: *Proceedings of the International Conference FGM IX*. American Institute of Physics, Oahu Island, Hawaii Melville, N.Y. 15–18 October 2006.
- Phan, C.N., Kardomateas, G.A., Frostig, Y., 2012a. Global buckling of a sandwich wide panel/beam based on the extended high order theory. *AIAA J.* 50 (8), 1707–1716 Aug.
- Phan, C.N., Bailey, N.W., Kardomateas, G.A., Battley, M.A., 2012c. Wrinkling of sandwich wide panels/beams based on the extended high order sandwich panel theory: formulation, comparison with elasticity and experiments. *Arch. Appl. Mech.* 82 (10–11), 1585–1599 (special Issue in Honor of Prof. Anthony Kounadis)October.
- Phan, C.N., Frostig, Y., Kardomateas, G.A., 2012b. Analysis of sandwich panels with a compliant core and with in-plane rigidity-extended high-order sandwich panel theory versus elasticity. *J. Appl. Mech. (ASME)* 79, 041001 (11 pages) 2012.
- Phan, C.N., Kardomateas, G.A., Frostig, Y., 2013. Blast response of a sandwich beam/wide plate based on the extended high-order sandwich panel theory (EHSAPT) and comparison with elasticity. *J. Appl. Mech. (ASME)* 80, 061005. doi:10.1115/1.4023619, 11 pages November 2013.
- Pijanka, J.K., Coudrillier, B., Ziegler, K., Sorensen, T., Meek, K.M., Nguyen, T.D., Quigley, H.A., Boote, C., 2012. Quantitative mapping of collagen fiber orientation in non-glaucoma and glaucoma posterior human sclera. *Investig. Ophthalmol. Vis. Sci.* 53 (9), 5258–5270.
- Plantema, F.J., 1966. *Sandwich Construction*. John Wiley and Sons, New York.
- Reddy, J.N., 1999. *Theory and Analysis of Elastic Plates*. Taylor and Francis, Philadelphia.
- Schwartz-Givli, H., Rabinovitch, O., Frostig, Y., 2007a. High order nonlinear contact effects in the dynamic behavior of delaminated sandwich panels with flexible core. *Int. J. Solids Struct.* 44 (1), 77–99.
- Schwartz-Givli, H., Rabinovitch, O., Frostig, Y., 2007b. High-order free vibrations of delaminated simply supported sandwich panels with a transversely flexible core – a modified galerkin approach. *J. Sound Vib.* 301 (1–2), 253–277.
- Sokolinsky, V., Frostig, Y., 2000. Branching behavior in the non-linear response of sandwich panels with a transversely flexible core. *Int. J. Solids Struct.* 37, 5745–5772.
- Suresh, S., Mortensen, A., 1998. *Fundamentals of Functionally Graded Materials: Processing and Thermomechanical Behavior of Graded Metals and Metal-Ceramic Composites*. IOM Communications Ltd, London.
- Venkataraman, S., Sankar, B.V., 2003. Elasticity solution for stresses in a sandwich beam with functionally graded core. *AIAA J.* 41 (12) December, pp. 2501–2250.
- Vinson, J.R., 1999. *The Behavior of Sandwich Structures of Isotropic and Composite Materials*. Technomic Publishing Co. Inc, Lancaster.
- Yuan, Z., Kardomateas, G.A., Frostig, Y., 2015. Finite element formulation based on the extended high order sandwich panel theory. *AIAA J.* 53 (10), 3006–3015 OCT 2015.